NSTX-U

Thermal Analysis of Neutral Beam Armor Array

NSTXU-CALC-11-05-00

September 22, 2011

Prepared By:

Kelsey Tresemer

Digitally signed by Kelsey Tresemer
DN: cn=Kelsey Tresemer, o=PPPL, ou=Mechanical Engineering, email=ktreseme@pppl.gov, c=US
Date: 2011.10.10 10:46:12 -04'00'

Kelsey Tresemer, Mechanical Engineer

Reviewed By:

Timothy N. Stevenson

Digitally signed by Timothy N. Stevenson
DN: cn=Timothy N. Stevenson, o=PPPL, ou=ENGR, email=tstevenson@pppl.gov, c=US
Date: 2011.10.10 12:03:56 -05'00'

Tim Stevenson, NSTX Neutral Beam Manager

Reviewed By:

Philip Heitzenroeder

Digitally signed by Philip Heitzenroeder
DN: cn=Philip Heitzenroeder, o=PPPL, ou=MED, email=pheitzen@pppl.gov, c=US
Date: 2011.10.10 14:13:11 -04'00'

Phil Heitzenroeder, Head, Mechanical Engineering

NSTXU-CALC-11-05-00

PPPL Calculation Form

Calculation # **NSTXU-CALC-11-05-00** Revision # **00** WP #, if any: **1707**
(ENG-032)

Purpose of Calculation: (Define why the calculation is being performed.)

- To confirm beam source profile fit on NB Armor face
- To calculate beam divergence and armor-incidence effect on beam heat flux magnitude
- To use calculated fluxes to establish fault conditions, testing armor for 1&2 beamline fault cases
- To confirm that the armor cooling system will be sufficient to remove any residual heat from the armor during normal NSTX-U operations.
- To examine stainless steel backing plates in terms of thermal expansion during bake out (@ 150°C) to ensure attached tiles to not interfere with each other.

References (List any source of design information including computer program titles and revision levels.)

- NSTX-U GRD (NB rev. 0 & CS rev. 3)
- Microsoft Excel
- ALGOR
- ProE

Assumptions (Identify all assumptions made as part of this calculation.)

- Assumed a 1.5 vertical and .5 horizontal, half-angle divergence from last scraping surface for each beamline source.
- Assumed a max temp for ATJ tiles of 2600°C. This reflects not a PHYSICAL limit, but rather one which avoids excessive sublimation of the carbon tiles.
- Assumed max tensile and compressive strengths of 26 MPa and 66MPa, respectively, for Graftech's ATJ graphite, as stated in their material properties sheet. (http://graftech.com/getattachment/800b4a74-3229-4e44-a4ff-7b212ab06e24/GRAFSTAR%E2%84%A2-ATJ%E2%84%A2-Graphite.asp)

Calculation (Calculation is either documented here or attached): Attached

Conclusion (Specify whether or not the purpose of the calculation was accomplished.):

Source fit on armor face: this was confirmed by physically modeling the source profiles after calculating the geometry changes to their shapes due to beam divergence and the smearing effects of the incident angles. It was confirmed that all six sources fit comfortably on the armor, albeit, with some overlapping effects.

Divergence and incident angle effects on heat flux magnitude: this was calculated and used to convert input powers of 80, 90, and 110 kV into applicable heat fluxes, useful for modeling fault conditions. It was found that the overall area of the beam profile increases significantly from the last scrape-off surface as the beam diverges and smears along the armor. This reduces the overall magnitude of the heat flux. Values were calculated for both individual sources as well as heat flux values for the overlapping areas. Source heat flux was split into "hotspot" and "outer ring" zones, where the power density was 80 and 20% total power, respectively.

Beamline fault conditions and testing: it quickly became clear that, in the case of a single BL fault, ATJ graphite was an adequate material to provide protection for the vacuum vessel wall. The surface temperature never exceeded 2000C, much less the limit of 2600C. The internal stresses at the T-bar slot shoulder were found to be sufficiently low, leading to the belief that there would be no threat of critical crack formation in that sensitive zone. The principle stresses in the bulk of the tile and on the surface were also found to be low, well within ATJ's published properties. If a single BL fault were to occur, the armor would survive without damage, barring any inherent weakness (unseen tile fractures, cracking). It would be recommended to attempt a visual inspection following the event as well as a complete maintenance event during the next outage.

However, for the double BL fault, the source overlap areas quickly exceeded ATJ graphite's limits for temperature and stress, generally passing this point after only 1/3 into the length of the shot. The main danger here is not so much the surface temperature, but the stress at the shoulder of the T-bar slot. If the shoulder cracks and detaches, the whole tile could fall from the armor, exposing the stainless steel backing plate to neutral particles and possibly causing damage to other internal NSTX-U fixtures. To remedy this, Carbon-Fiber Composite (CFC) will replace ATJ as the tile material in those zones. CFC possesses tensile strengths 3x that of ATJ as well as better thermal shock resistance. This material change will allow the armor to survive a double BL fault, probably with damage, but will allow the armor to successfully perform its duty as a sacrificial surface. As the fault strikes the armor, the tiles will rapidly heat, passing 2600C in 1/3 of the shot length. The tile surface will begin to rapidly sublimate, but not fast enough to pose any concern about completely eroding a tile. If a double BL event occurs, physical inspection of the armor array is strongly recommended and replacement of one or more tiles will be likely.

Between-shot cooling during normal operations: this analysis confirmed that the flow rate and diameter of the present cooling system will be more than adequate for the upgrade thermal loading during normal operations.

Thermal growth of backing plates under thermal loading: the ALGOR analysis showed that under normal thermal loading, the greatest of which occurs during bakeout, the stainless steel backing plates grow "up and out" away from each other. Therefore, thermal loading of the plates poses no threat to the graphite/CFC tiles and the array will be able to flex and grow freely as it heats up during bakeout.

Cognizant Engineer's printed name, signature, and date

Kelsey Tresemer — Digitally signed by Kelsey Tresemer
DN: cn=Kelsey Tresemer, o=PPPL, ou=Mechanical Engineering, email=ktreseme@pppl.gov, c=US
Date: 2011.10.10 14:01:41 -04'00'

I have reviewed this calculation and, to my professional satisfaction, it is properly performed and correct.

Checker's printed name, signature, and date

Timothy N. Stevenson — Digitally signed by Timothy N. Stevenson
DN: cn=Timothy N. Stevenson, o=PPPL, ou=ENGR, email=tstevenson@pppl.gov, c=US
Date: 2011.10.10 13:07:14 -05'00'

Calculation

Introduction:

The Neutral Beamline Injection System (NBIS) Armor serves as a sacrificial protective surface for the neutral beamlines (NBs). With the addition of a second beamline, the armor went through a review and analysis to evaluate its performance with this increase to its mechanical and thermal requirements.

The upgrade proposal features the armor's counterclockwise movement inside the vacuum vessel to allow both sets of neutral beamline (NB) profiles to fit on the armor face. The beamlines overlap, causing areas of considerably increased heat flux, which were then analyzed for normal operations and fault conditions using simple tile shapes in ALGOR. The cooling lines were also analyzed for normal operational cooling with a simple simulation in ALGOR. Finally, the backing plates were analyzed to ensure that thermal growth during bakeout would not cause any interference between quadrants. The armor's mechanical capabilities were analyzed under a separate calculation.

Explanation of Excel Calculation Sheet:

This portion of the NB armor calculation covers the NB source profiles, their mapping and the effect of the source divergence and surface smearing on the magnitude of the source heat flux. The heat flux gradients were also calculated in this file.

Sheet 1: Determining Divergence in NBI 1 & 2

The origin of the source was assumed to be from the last scrape-off surface, causing the source profile to assume a rectangular shape, 4.72 in by 17.32 in (12 cm by 44 cm), with area of 81.84 in^2 (528 cm^2). The distances between the last scrape-off surface and the face of the NBI armor array was measured via ProE for each BL source. From this, assuming the vertical and horizontal half-angle beam divergence of 1.5 and .5, respectively, the change in overall source profile dimensions was calculated, and the ratio of new area to old noted.

EXAMPLE: Δ in total dimension = distance from scrapeoff(tan (2*halfangle))

$$\Delta d_{total} = 311.521 * \tan(2*(0.5))$$
$$\Delta d_{total} = 5.437$$

This is then added to the original dimension, resulting in the final horizontal and vertical size.

Sheet 2: Source "Smear"

As the beamline sources encounter the face of the armor, the incidence angle acts as a "smearing" surface, horizontally enlarging the source profile area. The diverged values from sheet 1 were run though this calculation which produced a new, "smeared" number for the horizontal dimension. The incident angle causes no vertical "smearing".

EXAMPLE: "smear" width = original width/sin(incidence angle)

$$w_{smear} = w_o / \sin(\theta)$$
$$w_{smear} = 10.162 / \sin(68.7°)$$
$$w_{smear} = 10.907$$

This sheet also contains the calculation which created the inner zone to the source profile. Rather than model the power distribution as a double Gaussian curve, a 20% reduction in size was estimated to contain 80% of the beam's power, and was thusly modeled.

Sheet 3: Source profile confirmation via photo data

In order to confirm the mathematical assumptions up until this point, the data from the sheets 1&2 were coMPared with photos taken of the NB armor, post-run. By measuring the areas where lithium was NOT deposited, we can get an idea of the total size and dimension of the source profile. Lithium evaporates at around

600 C, a number which coordinated to the hottest part of the source profile (or the 80% of the source). CoMParisons showed that the mathematical assumptions were ~8% larger than the photograph.

Sheet 4: Ellipse Conversion

The true shape of the source profile as it encounters the armor is an ellipse, caused by divergence. Up until this point, the calculated dimensions have been simply the vertical height and the horizontal width of the profile. To properly represent the source shape, these values needed to be converted into an elliptical shape. Sheet 3 showed that ellipses created with these values will be 8% larger than in reality, which will affect the ultimate outcome of this analysis.

Formula for the area of an ellipse: $\pi ab, where\ a\ and\ b\ are\ \frac{1}{2}\ the\ width\ and\ height, respectively$

By taking a ratio of the area of the source profile at the last scrape-off surface (81.84 in^2) and the elliptical area of the source profile as it encounters the armor face, after it has experienced divergence and smearing, a value was obtained to manipulate the magnitude of the beamline's heat flux.

$$q_{scrape\ off}\left({}^{MW}/_{m^2}\right){}^{A_0}/_{A_1} = q_{armor\ face}$$

This sheet also addresses the issue of when a source strikes the intersection of the two armor halves. This would cause the source profile to encounter two, different, incident angles, smearing the profile accordingly. To model these shapes in ProE, each portion of the source, or remnant, was treated as an entire unit, and smeared as per its respective angle. The profiles were applied to a global model of the NBI armor and the excess beam source trimmed away. The final width of each portion of source was recorded on this sheet.

At this point, the source profiles were applied to an armor model to confirm fit. Apart from some source overlap, all six profiles fit comfortably on the armor's face.

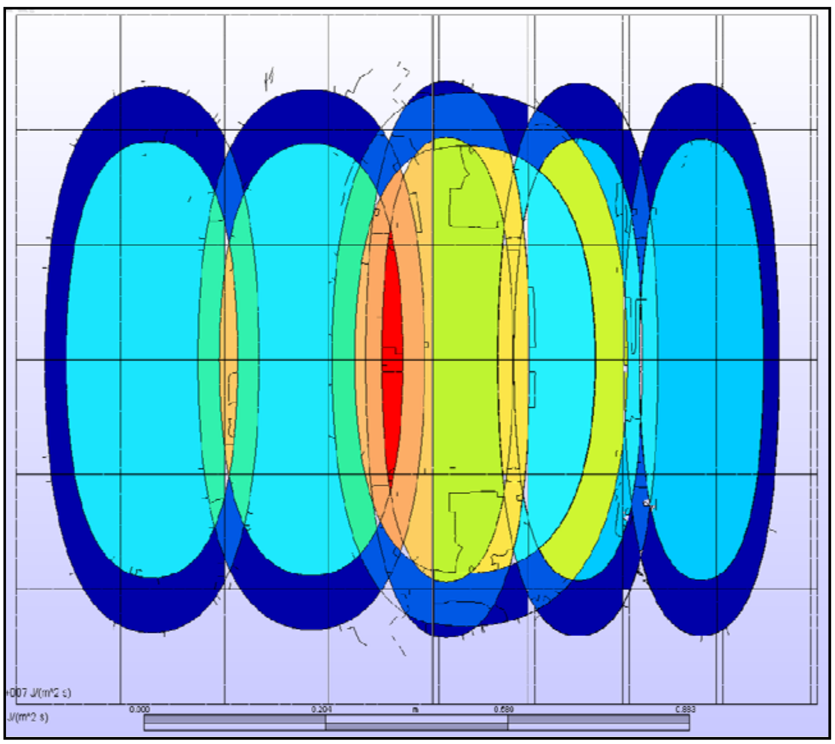

Figure 1. Confirming source profile fit on armor face

Sheet 5: Heat Flux Magnitude

This sheet contains the calculation to apply the changes to the beam source profiles to the magnitude of the heat flux. At the last scraping surface, the heat flux per source is the equivalent to the source power (as defined by the shot parameters) divided by the area of the source. This heat flux was further broken down into 80% and 20% portions, to represent the hot spot and outer ring of power densities.

For a 5 sec, 5MW shot:

$$\frac{5\ MW}{3\ sources} = 1.67\ MW$$

$$\frac{1.67\ MW}{81.84\ in^2} = 3.16\text{E}07\ \ MW/in^2$$

$$.80 * 3.16\text{E}07 = \ 2.35\text{E}07\ \ MW/in^2$$
$$.20 * 3.16\text{E}07 = \ 6.31\text{E}06\ \ MW/in^2$$

From sheet 2, it was found that the source profiles experience both divergence and smearing, meaning that the source profile, when applied the face of the armor, increases in size. By taking a ratio of A_0/A_1, we can use this to modify the source profile's heat flux at the last scraping surface, and attain the at-armor-face heat flux.

$$\frac{A_0}{A_1} = \frac{81.84in^2}{264.46in^2} = \ .305$$

$$(80\%)\ \ 2.35\text{E}07\ \ MW/in^2 * \ .305 = \ 7.698\text{E}06\ \ MW/in^2$$
$$(20\%)\ \ 6.34\text{E}06\ \ MW/in^2 * \ .305 = \ 1.925\text{E}06\ \ MW/in^2$$

Once these numbers were calculated for the hot spots and the outer rings, the overlap areas were identified using the ProE model of the armor and their respective heat flux magnitudes were computed. An area of particular concern is #7, where three hot spots converge: BL2 B, BL2 A2, and BL1 C2.

Explanation of ALGOR analysis:

Once the heat fluxes for the armor were determined, it was then possible to construct scenarios for normal operations and possible fault conditions. During normal operation, the armor would see the same level of heat deposition as the rest of the First Wall devices, approximately .06 MW/m^2 average with .13 MW/m^2 peaking. This is very low-level heating and the armor would be under no threat of damage.

The fault conditions were split into two cases: single beam and double beam. A single beam fault would be the event in which a single beam fired into the armor in the absence of plasma in the vessel. The duration of such an event would be anywhere from a fraction of a second to 5 seconds. The magnitude of the applied heat flux would vary widely, with worst cases of 7.6 MW/m^2, 9.1 MW/m^2, and 13.6 MW/m^2 for 80, 90, and 110 kV, respectively. A double beam fault could see heat flux magnitudes of up to three times these values in areas of source overlap.

Assumptions:

Default nodal temperature: 20C
Ambient Temperature (for radiation): 60C
Element: Brick
Modeled with bricks and tetrahedrons
Material: ATJ graphite (material data file attached to Armor Analysis Excel file)

A single armor tile was modeled in ProE and, due to surface requirements of ALGOR, its top surface was sectioned to allow different heat flux values to be applied to different areas. This allowed the use of a single model for both single and double BL fault analyses. In ALGOR, the heat flux values generated in sheet 5 of the Excel analysis. For a single beamline fault, the entire surface of the tile was applied with the heat flux from source BL1 C2 (highest heat flux of the six), for 80, 90, and 110 kV shots, for 5, 3, and 1 seconds long, respectively. This represented the "worst case" of the single BL faults. Radiation was enabled on the top surface as well (emissivity of 0.3). Each shot was allowed to run for the full time length and the max temperature and subsequent stresses recorded.

Table 1. ALGOR Single BL Fault Results

	time to 2600C	VonMises @ 2600C (T-bar slot) MPa	Max Principle @ 2600 (overall) MPa	Time to 26 MPa	Related Max Principle MPa	Temp at 26 MPa (VM) C
1 BL						
80 kV	5.05s: 1781.40	15.88	13.19	x	x	x
90 kV	3.08s: 1581.25	16.66	12.48	x	x	x
110 kV	1.05s: 1285.10	18.43	11.29	x	x	x

A double BL fault utilized the sections cut into the surface and focused attention on the armor tile which was exposed to the greatest heat flux: tile C4. The heat flux applied to this tile corresponded with the overlap heat fluxes 4-9, listed on sheet 5 of the Excel analysis. Each of these heat fluxes were assigned to a section on the tile surface, with radiation enabled across the top surface as well (emissivity of 0.3). Runs were made of 80, 90, and 110 kV heat fluxes, in an attempt to see how long before the tile surface a) reached 2600C and b) the internal stresses reached the limit of 26 MPa (tension).

Table 2. ALGOR Double BL Fault Results

	time to 2600C	VonMises @ 2600C (T-bar slot) MPa	Max Principle @ 2600 (overall) MPa	Time to 26 MPa	Related Max Principle MPa	Temp at 26 MPa (VM) C
2 BL						
80 kV	2.44s: 2610.55	31.91	20.02	1.63s: 25.90 MPa	15.59	2083.65
90 kV	1.73s: 2616.67	34.9	20.59	.978s: 25.82 MPa	14.47	1944.84
110 kV	.740s: 2601.23	37.53	21.36	.383s: 25.16 MPa	14.77	1804

Cooling Line Evaluation

In order to evaluate the efficiency of the cooling lines imbedded into the stainless steel backing plates, a simple test piece was constructed to find the thermal time constant (T_c) of the system, or, rather, to find the time it took for 63% of the heat in the system to be removed by the cooling system. A test piece was assembled in ProE which was a slice of ATJ tile, stainless steel backing plate, and embedded copper tube. In ALGOR, an initial temperature significantly higher than any the system would see during normal operations was applied to the entire assembly (1000C). The conditions of the cooling system were applied to the copper tube (3/8" dia., 3.6 GPM per backing plate) and the system left to run. The resulting graph was created and the time constant easily found: ~50s.

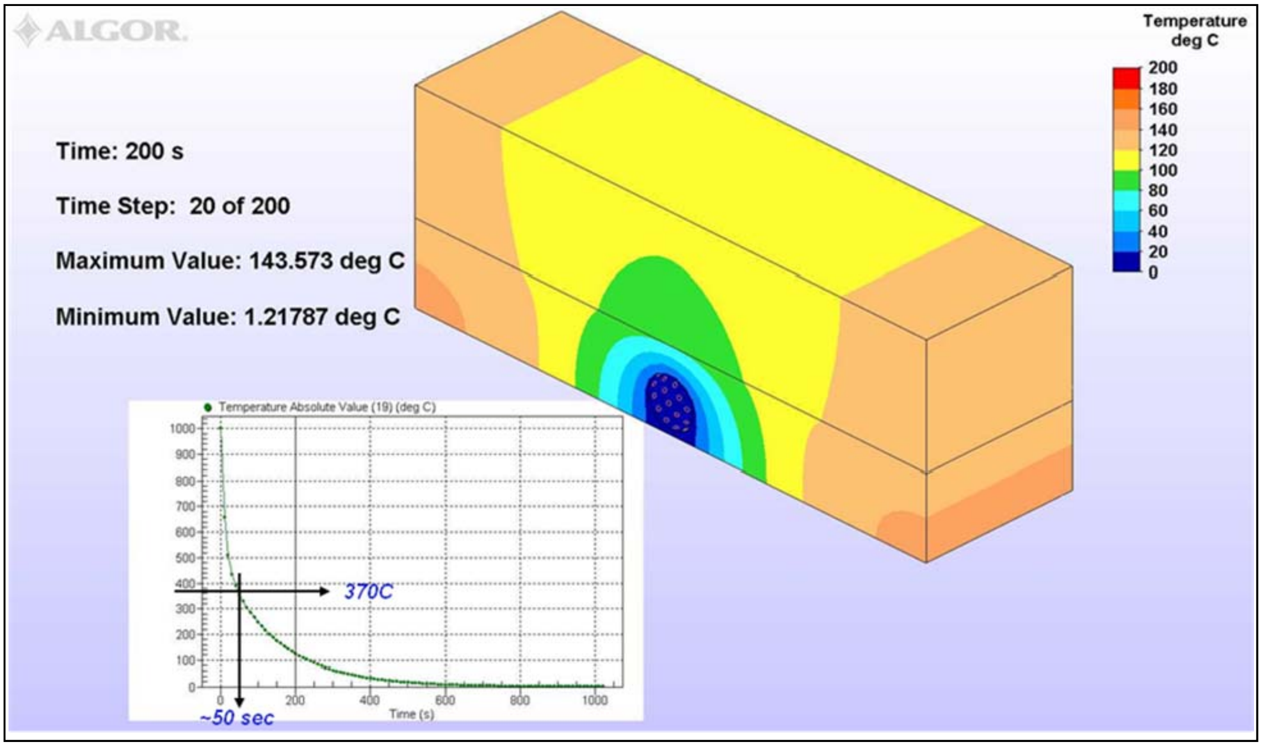

Figure 2. ALGOR results of cooling line analysis.

This is simply an estimate in order to gain a perspective on how quick the majority of the heat within the armor can be removed. Since during normal operations the armor will only see a net heat gain of a few hundred degrees Celsius, as well as a between-shot cooling period of nearly 20 minutes, it is safe to deem the system adequate for use in NSTX-U.

Backing Plate Thermal Growth

The mounting points for the armor underwent significant design changes, prompting an analysis of the armor's constraints and the manner in which it would mechanically respond to thermal loading. Since the amor array is symmetric about the horizontal and vertical axes, only a single quadrant's backing plate needed analysis. The plate was modeled in ProE and uploaded to ALGOR for testing. Since the highest temperatures the armor should ever see in normal operations would be during bake out, those conditions were simulated for the test. Hot helium was flowed through the cooling lines until the whole part reached ~350C and the consequent thermal growth was monitored and recorded. There was a chance that the plates could thermally grow towards one another, causing tile interference and possible fracturing and this needed confirmation.

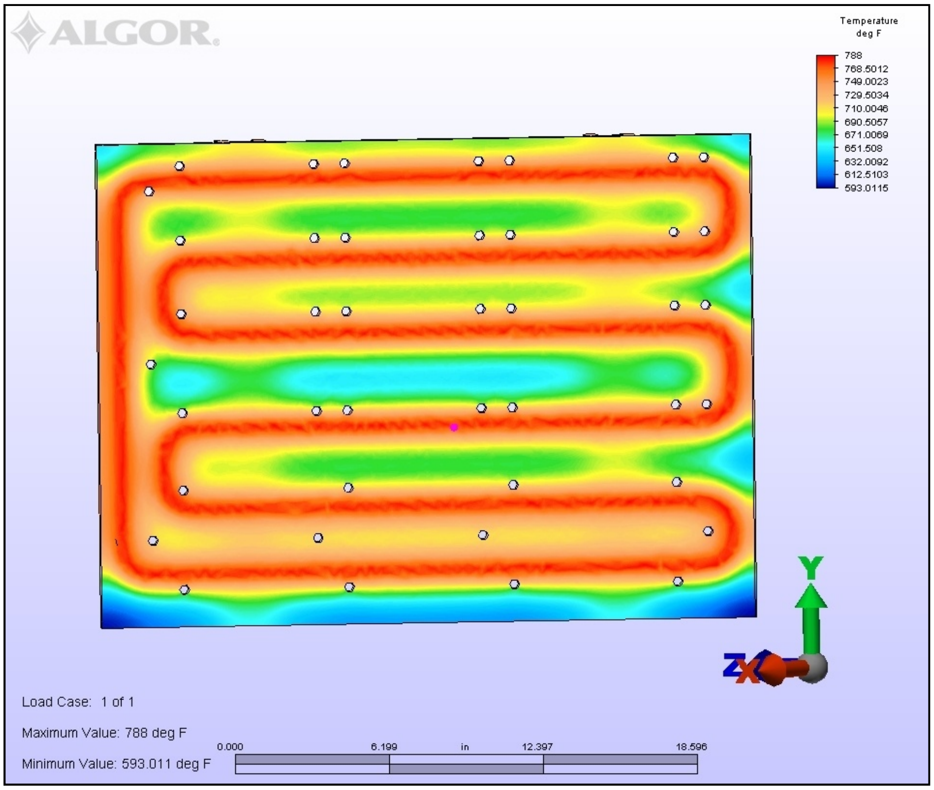

Figure 3. ALGOR analysis of stainless steel backing plate thermal growth during bakeout: thermal heating

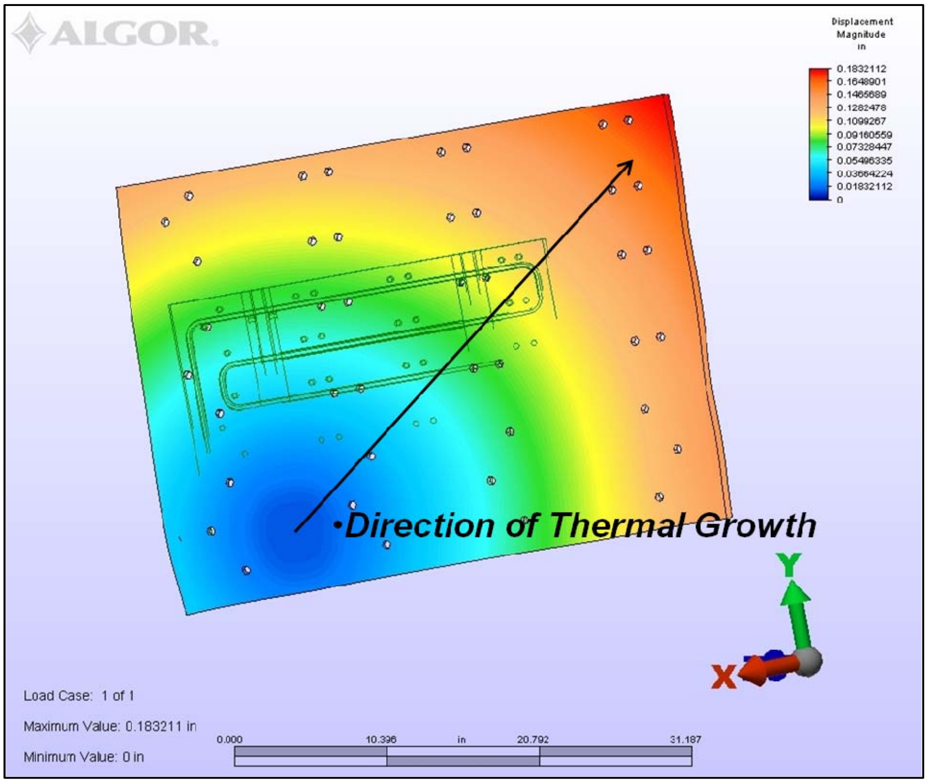

Figure 4. ALGOR analysis of stainless steel backing plate thermal growth during bakeout: mechanical growth

Conclusion

Source fit on armor face: this was confirmed by physically modeling the source profiles after calculating the geometry changes to their shapes due to beam divergence and the smearing effects of the incident angles. It was confirmed that all six sources fit comfortably on the armor, albeit, with some overlapping effects.

Divergence and incident angle effects on heat flux magnitude: this was calculated and used to convert input powers of 80, 90, and 110 kV into applicable heat fluxes, useful for modeling fault conditions. It was found that the overall area of the beam profile increases significantly from the last scrape-off surface as the beam diverges and smears along the armor. This reduces the overall magnitude of the heat flux. Values were calculated for both individual sources as well as heat flux values for the overlapping areas. Source heat flux was split into “hotspot” and “outer ring” zones, where the power density was 80 and 20% total power, respectively.

Beamline fault conditions and testing: it quickly became clear that, in the case of a single BL fault, ATJ graphite was an adequate material to provide protection for the vacuum vessel wall. The surface temperature never exceeded 2000C, much less the limit of 2600C. The internal stresses at the T-bar slot shoulder were found to be sufficiently low, leading to the belief that there would be no threat of critical crack formation in that sensitive zone. The principle stresses in the bulk of the tile and on the surface were also found to be low, well within ATJ’s published properties. If a single BL fault were to occur, the armor would survive without damage, barring any inherent weakness (unseen tile fractures, cracking). It would be recommended to attempt a visual inspection following the event as well as a complete maintenance event during the next outage.

However, for the double BL fault, the source overlap areas quickly exceeded ATJ graphite’s limits for temperature and stress, generally passing this point after only 1/3 into the length of the shot. The main danger here is not so much the surface temperature, but the stress at the shoulder of the T-bar slot. If the shoulder cracks and detaches, the whole tile could fall from the armor, exposing the stainless steel backing plate to neutral particles and possibly causing damage to other internal NSTX-U fixtures. To remedy this, Carbon-Fiber Composite (CFC) will replace ATJ as the tile material in those zones. CFC possesses tensile strengths 3x that of ATJ as well as better thermal shock resistance. This material change will allow the armor to survive a double BL fault, probably with damage, but will allow the armor to successfully perform its duty as a sacrificial surface. As the fault strikes the armor, the tiles will rapidly heat, passing 2600C in 1/3 of the shot length. The tile surface will begin to rapidly sublimate, but not fast enough to pose any concern about completely eroding a tile. If a double BL event occurs, physical inspection of the armor array is strongly recommended and replacement of one or more tiles will be likely.

Between-shot cooling during normal operations: this analysis confirmed that the flow rate and diameter of the present cooling system will be more than adequate for the upgrade thermal loading during normal operations.

Thermal growth of backing plates under thermal loading: the ALGOR analysis showed that under normal thermal loading, the greatest of which occurs during bakeout, the stainless steel backing plates grow “up and out” away from each other. Therefore, thermal loading of the plates poses no threat to the graphite/CFC tiles and the array will be able to flex and grow freely as it heats up during bakeout.

Appendix A: Excel Analysis

Excel Sheet 1

Determining Divergence in NB1 and NB2

Current Beam Line

Constants	in	cm			in^2	cm^2
beam w	4.724409	12		Area	81.84016	528
beam h	17.32283	44				

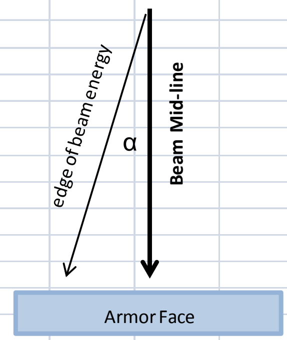

Divergence (in deg)

Δ in total dimensions (using 2α)

			BL1 (inches)		BL1 (cm)	
α Horiz.						
0.5	Dist: scrape to armor		Horz. (x)	Vert. (y)	Horz. (x)	Vert. (y)
α Vert.	B_1A	311.521	5.437	16.315	13.8105	41.43992
1.5	B_1B	312.359	5.452	16.359	13.84765	41.55139
	B_1C	316.266	5.520	16.563	14.02086	42.07112

		BL2 (inches)		BL2 (cm)	
Dist: scrape to armor		Horz.	Vert.	Horz.	Vert.
B_2A	290.349	5.068	15.206	12.87189	38.62353
B_2B	297.931	5.200	15.603	13.20802	39.63212
B_2C	304.572	5.316	15.951	13.50243	40.51553

Final dimensions

	inches			cm			A_0/A_1	A_1/A_0
	beam w	beam h		beam w	beam h			
B_1A	10.162	33.638	B_1A	25.811	85.440	B_1A	0.30485	3.280297
B_1B	10.176	33.682	B_1B	25.848	85.551	B_1B	0.304016	3.289305
B_1C	10.244	33.886	B_1C	26.021	86.071	B_1C	0.300168	3.331463
B_2A	9.792	32.529	B_2A	24.872	82.624	B_2A	0.327138	3.056811
B_2B	9.924	32.926	B_2B	25.208	83.632	B_2B	0.318884	3.135941
B_2C	10.040	33.274	B_2C	25.502	84.516	B_2C	0.311908	3.206078

Excel Sheet 2

Determining Beam Smear On Armor Face

Current Beam Line

Constants	in	cm			in^2	cm^2
beam w	4.724	12				
beam h	17.323	44	Area	81.84016368	528	

	inches				cm	
	beam w	beam h			beam w	beam h
B1A	10.162	33.638		B1A	25.811	85.440
B1B	10.176	33.682		B1B	25.848	85.551
B1C	10.244	33.886		B1C	26.021	86.071
B2A	9.792	32.529		B2A	24.872	82.624
B2B	9.924	32.926		B2B	25.208	83.632
B2C	10.040	33.274		B2C	25.502	84.516

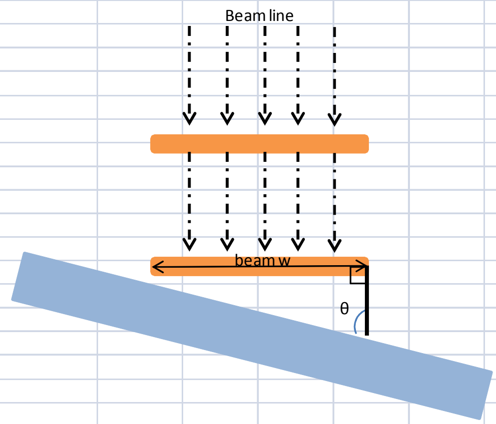

	Beam Line	Incidence Angle (θ)	smear width	height	A_0/A_1	smear width	height
			inches			cm	
BL1	B_1A	68.7	10.91	33.638	0.284	27.703	85.440
	B_1B	64.7	11.26	33.682	0.275	28.590	85.551
	B_1C_1	60.7	11.75	33.886	0.262	29.838	86.071
	B_1C_2	94.3	10.27	33.886	0.299	26.094	86.071
BL2	B_2A_1	25.6	22.66	32.529	0.141	57.562	82.624
	B_2A_2	39.4	15.43	32.529	0.208	39.185	82.624
	B_2B	43.4	14.44	32.926	0.219	36.688	83.632
	B_2C	47.4	13.64	33.274	0.230	34.645	84.516

Adjust number for a 20% reduction in size to represent inner "hotspot" (80% total power)

	Beam Line	width	height	smear width	height
		inches		cm	
BL1	B_1A	8.725	26.910	22.162	68.352
	B_1B	9.005	26.945	22.872	68.441
	B_1C_1	9.398	27.109	23.870	68.857
	B_1C_2	8.219	27.109	20.875	68.857
BL2	B_2A_1	18.130	26.023	46.050	66.099
	B_2A_2	12.342	26.023	31.348	66.099
	B_2B	11.555	26.341	29.351	66.906
	B_2C	10.912	26.619	27.716	67.612

*We assume that power density falls off at the edges of the beam line due to divergence in the beam. A 20-80 division has been accepted as a model of power density.

Excel Sheet 3

Photo Confirmation of Beam Spread

From Smear Page:
beam h 26.91021

From Photo:
beam h 24.84243

% Difference:
7.990997
(About 8% too large of an ellipse)

Beam height
24.84243 inches

in photo
5.125 inches

Tile Height
27.872 inches

in photo
5.75 inches

Excel Sheet 4

Ellipse Conversion

*If a source hits TWO of the armor faces, the beam experiences different smearing effects, depending on the incident angle.
Sources needed to be split into two pieces, one for each armor side, and analyzed separately.

Current Beam Line

Constants	in	cm
beam w	4.724	12
beam h	17.323	44

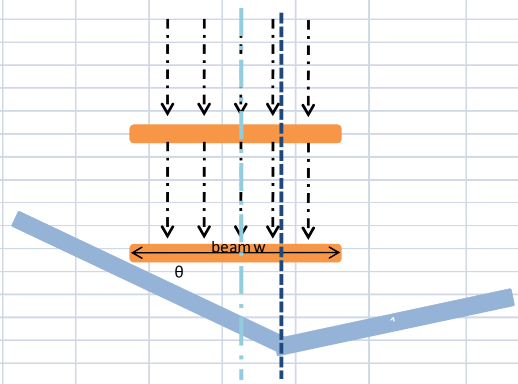

	Beam Line	width	height	smear width	height
		inches		cm	
BL1	B1A	8.725	26.910	22.162	68.352
	B1B	9.005	26.945	22.872	68.441
	B1C1	9.398	27.109	23.870	68.857
	B1C2	8.219	27.109	20.875	68.857
BL2	B2A1	18.130	26.023	46.050	66.099
	B2A2	12.342	26.023	31.348	66.099
	B2B	11.555	26.341	29.351	66.906
	B2C	10.912	26.619	27.716	67.612

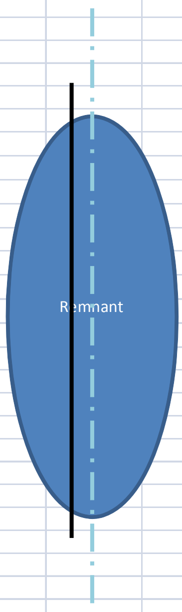

	Beam Line	Incidence Angle (θ)	beam dimensions after diverg		Smear Dimensions		Remnant Width (measured)
			beam w	beam h	width	height	
BL1	B_1A	68.7	10.162	33.638	10.907	33.638	
	B_1B	64.7	10.176	33.682	11.256	33.682	
	B_1C_1	60.7	10.244	33.886	11.747	33.886	6.739
	B_1C_2	94.3	10.244	33.886	10.273	33.886	4.236
BL2	B_2A_1	25.6	9.792	32.529	22.662	32.529	13.612
	B_2A_2	39.4	9.792	32.529	15.427	32.529	6.379
	B_2B	43.4	9.924	32.926	14.444	32.926	
	B_2C	47.4	10.040	33.274	13.640	33.274	

NSTXU-CALC-11-05-00

Excel Sheet 5

Heat Flux Per Tile

	1	2	3	4	5	6	7	8
A								
B								
C								
D								
E								
F								

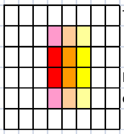

Time (sec)	
	0.75
FAULT	
q (heat flux W/m^2)	
	3.79E+07
HotSpot (80%)	
	3.03E+07
OuterRing(20%)	
	7.58E+06

		A_0/A_1	HS power (W/m^2)	OD power (W/m^2)
BL1	B1A	0.284	8.607E+06	2.152E+06
	B1B	0.275	8.329E+06	2.082E+06
	B1C1	0.262	7.932E+06	1.983E+06
	B1C2	0.299	9.070E+06	2.268E+06
BL2	B2A1	0.141	4.283E+06	1.071E+06
	B2A2	0.208	6.292E+06	1.573E+06
	B2B	0.219	6.639E+06	1.660E+06
	B2C	0.230	6.957E+06	1.739E+06

Overlap heat fluxes

1	8.617E+06	2CHS + 2BOD
2	1.360E+07	2CHS + 2BHS
3	8.379E+06	2COD+ 2BHS
4	8.212E+06	2BHS + 2A2OD
5	8.617E+06	2BHS + 2A2HS
6	1.520E+07	2BHS + 2A2HS + 1C2OD
7	2.200E+07	2BHS + 2A2HS + 1C2HS
8	1.702E+07	2BOD + 2A2HS + 1C2HS
9	1.536E+07	2A2HS + 1C2HS
10	1.222E+07	2A1HS + 1C1HS
11	1.430E+07	2A1HS + 1C1HS + 1BOD
12	1.460E+07	2A1HS + 1C1OD + 1BHS
13	6.366E+06	2A1HS + 1BOD
14	1.261E+07	2A1HS + 1BHS
15	9.400E+06	2A1OD + 1BHS
16	1.048E+07	1BHS + 1AOD
17	1.069E+07	1BOD + 1AHS

NBI Power to Plasma/Beam line

	Pulse Length (s)	Power to plasma (MW)	2 NB	power/source (MW)	q (per source, W/m^2)	
	5.00	5	10	1.67	3.16E+07	80 kV
	4.00	5.4	10.8	1.80	3.41E+07	
0.0528	3.00	6	12	2.00	3.79E+07	90 kV
	2.00	6.8	13.6	2.27	4.29E+07	
	1.50	7.5	15	2.50	4.73E+07	
	1.25	8.2	16.4	2.73	5.18E+07	
	1.00	9	18	3.00	5.68E+07	110 kV

MSE	power/source (MW)	q (per source, W/m^2)
	1.67	1.40E+07
	2.00	1.90E+07
	3.00	2.80E+07

Excel Sheet 6

ALGOR results

	time to 2600C	VonMises @ 2600C (tbar slot) Mpa	Max Principle @ 2600 (overall) Mpa	Time to 26 Mpa	Related Max Principle Mpa	Temp at 26 MPa (VM) C
1 BL						
80 kV	5.05s: 1781.40	15.88	13.19	x	x	x
90 kV	3.08s: 1581.25	16.66	12.48	x	x	x
110 kV	1.05s: 1285.10	18.43	11.29	x	x	x
	time to 2600C	VonMises @ 2600C (tbar slot) Mpa	Max Principle @ 2600 (overall) Mpa	Time to 26 Mpa	Related Max Principle Mpa	Temp at 26 MPa (VM) C
2 BL						
80 kV	2.44s: 2610.55C	31.91	20.02	1.63s: 25.90 Mpa	15.59	2083.65
90 kV	1.73s: 2616.67C	34.9	20.59	.978s: 25.82 Mpa	14.47	1944.84
110 kV	.740s: 2601.23	37.53	21.36	.383S: 25.16 Mpa	14.77	1804

Excel Sheet 7

	Temp ©	kx	ky	kz	Sp					
	0	116	116	116	711		k = thermal conductivity (W/mk)			
	27	116	116	116	711					
	127	106	106	106	975					
	227	95	95	95	1185					
	527	75	75	75	1600					
	1027	50	50	50	1865					
	1527	43	43	43	1975					
	2027	42	42	42	2050					
	2627	40	40	40	2060					
	3027	40	40	40	2075					

Appendix B: ALGOR Results

80 kV, 5s

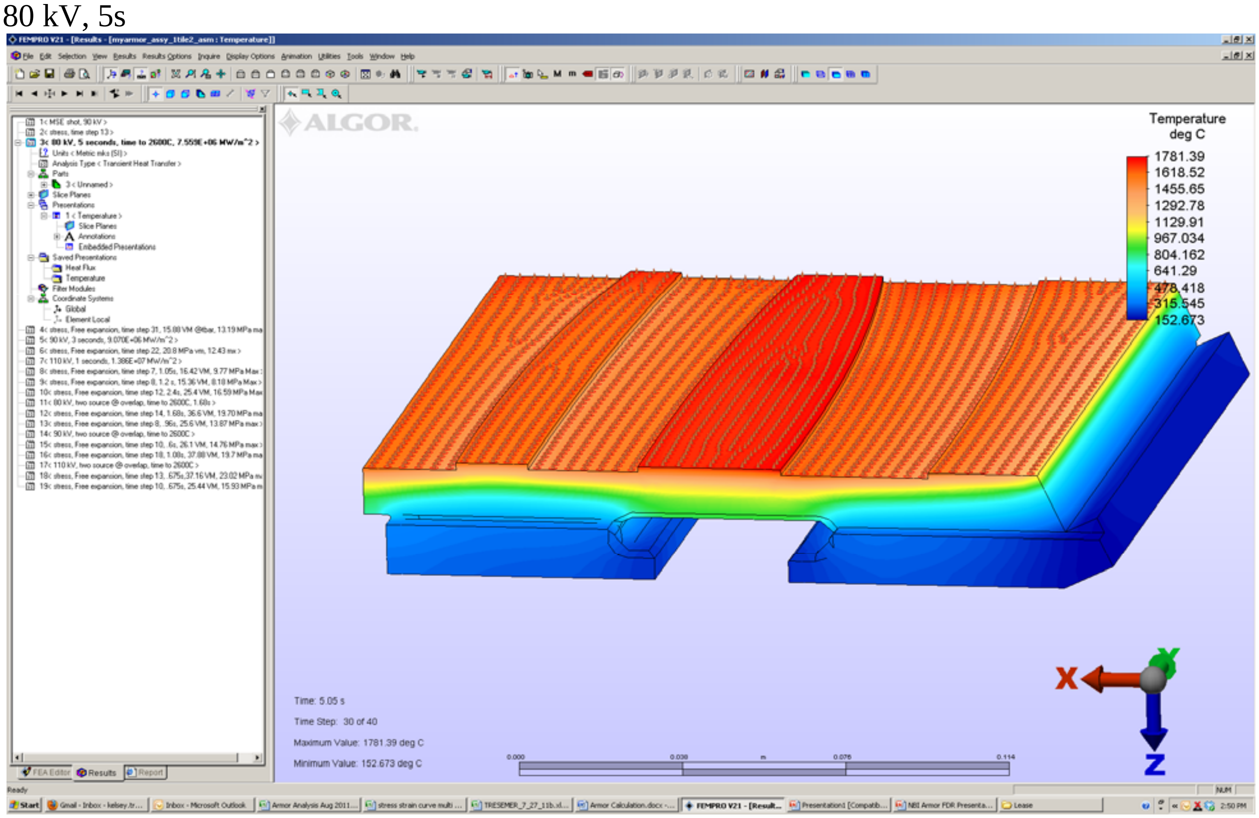

80 kV Von Mises Stress

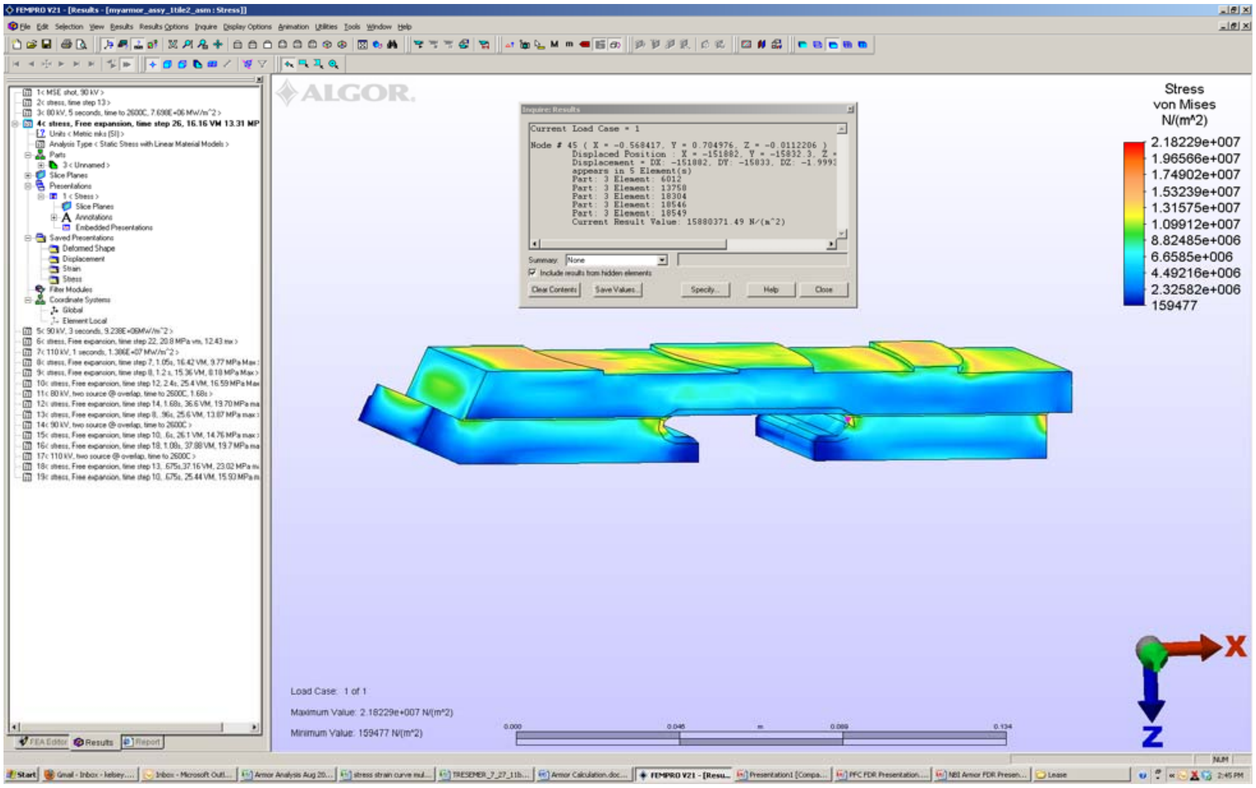

80 kV Max Principle Stress

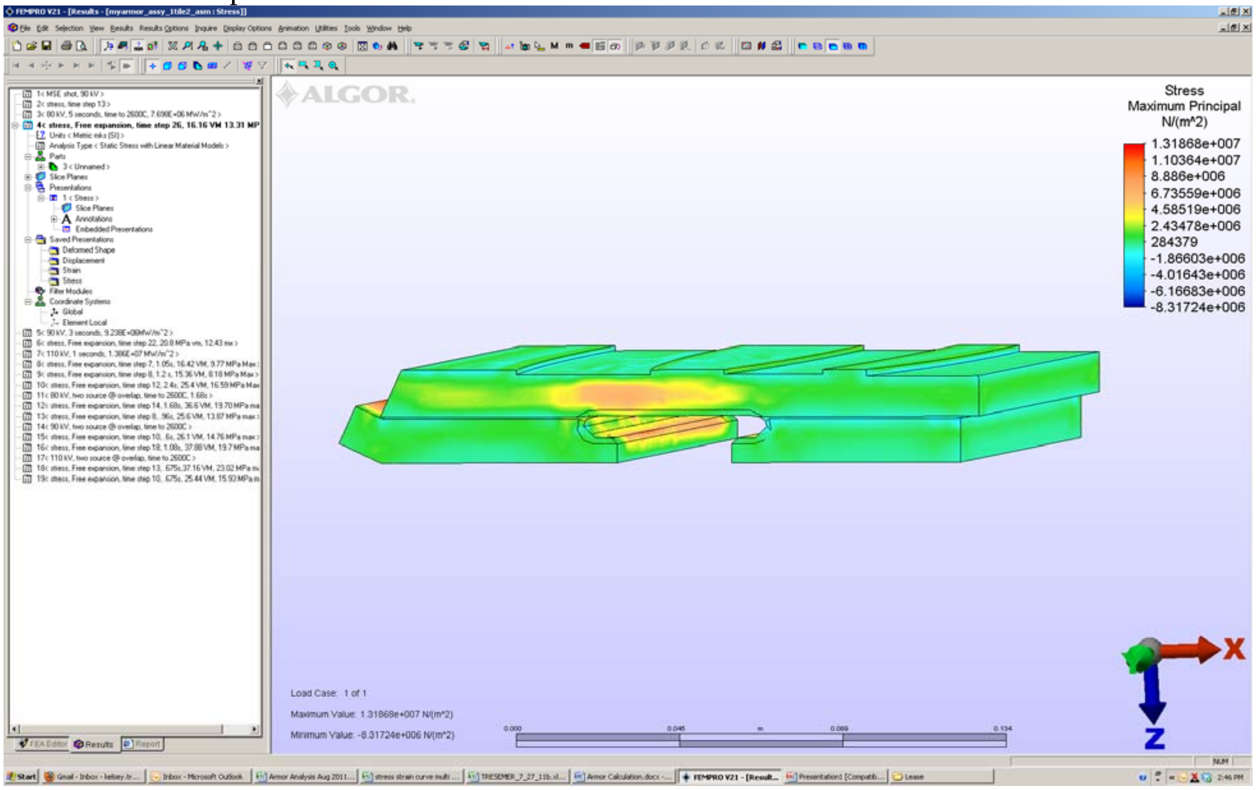

90 kV, 3s

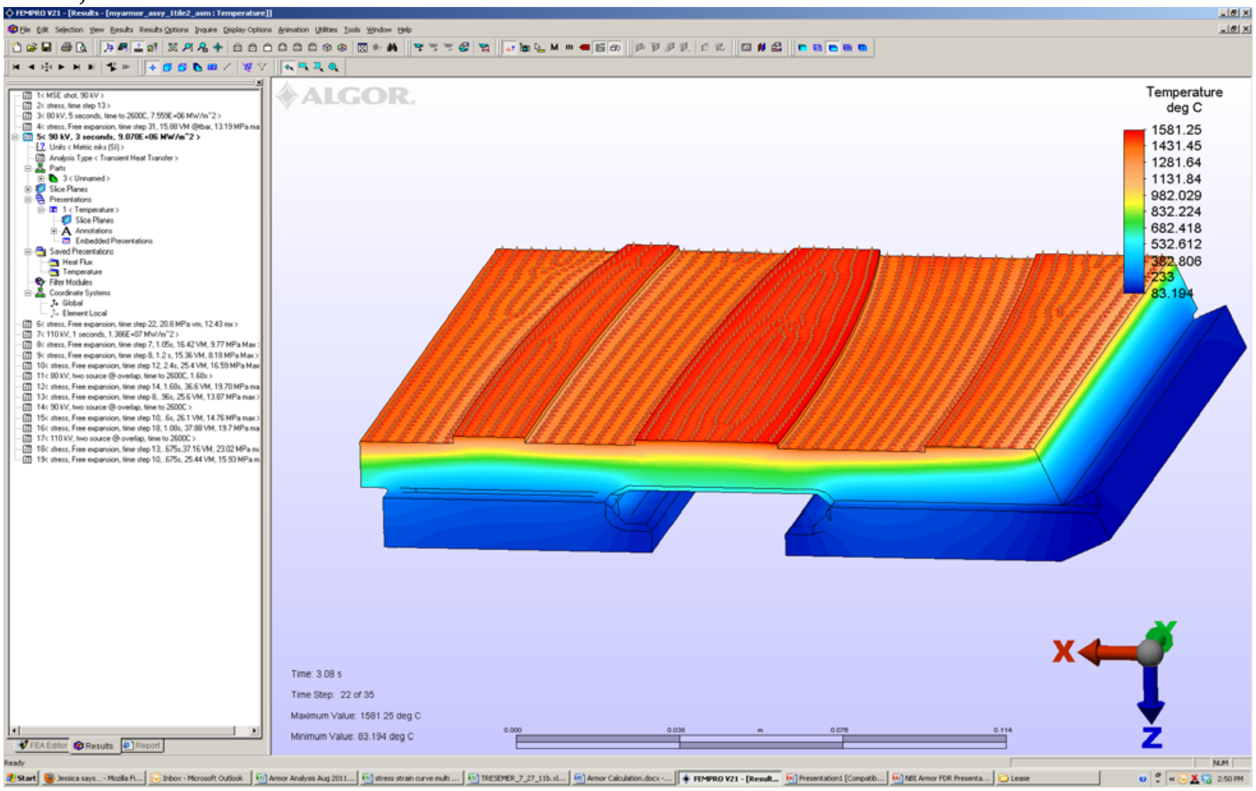

90 kV Von Mises Stress

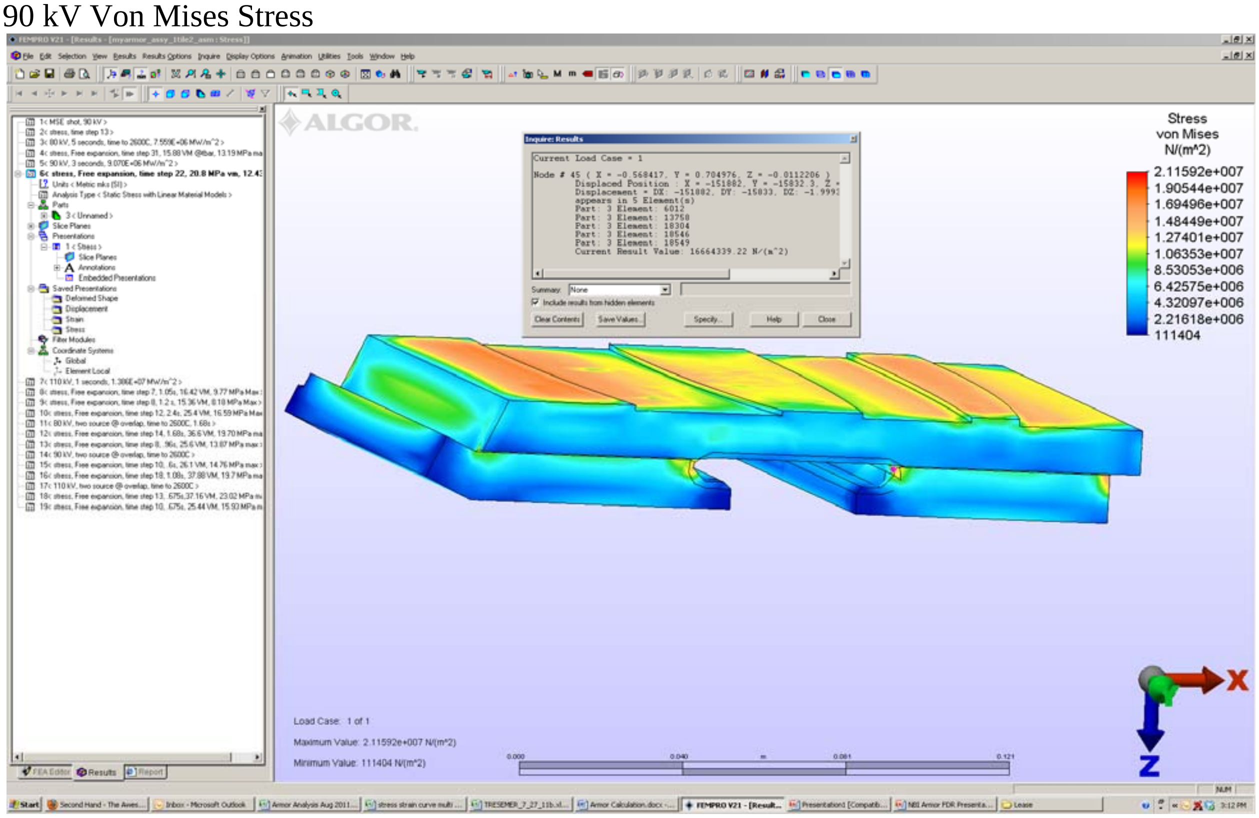

90 kV Max Principle Stress

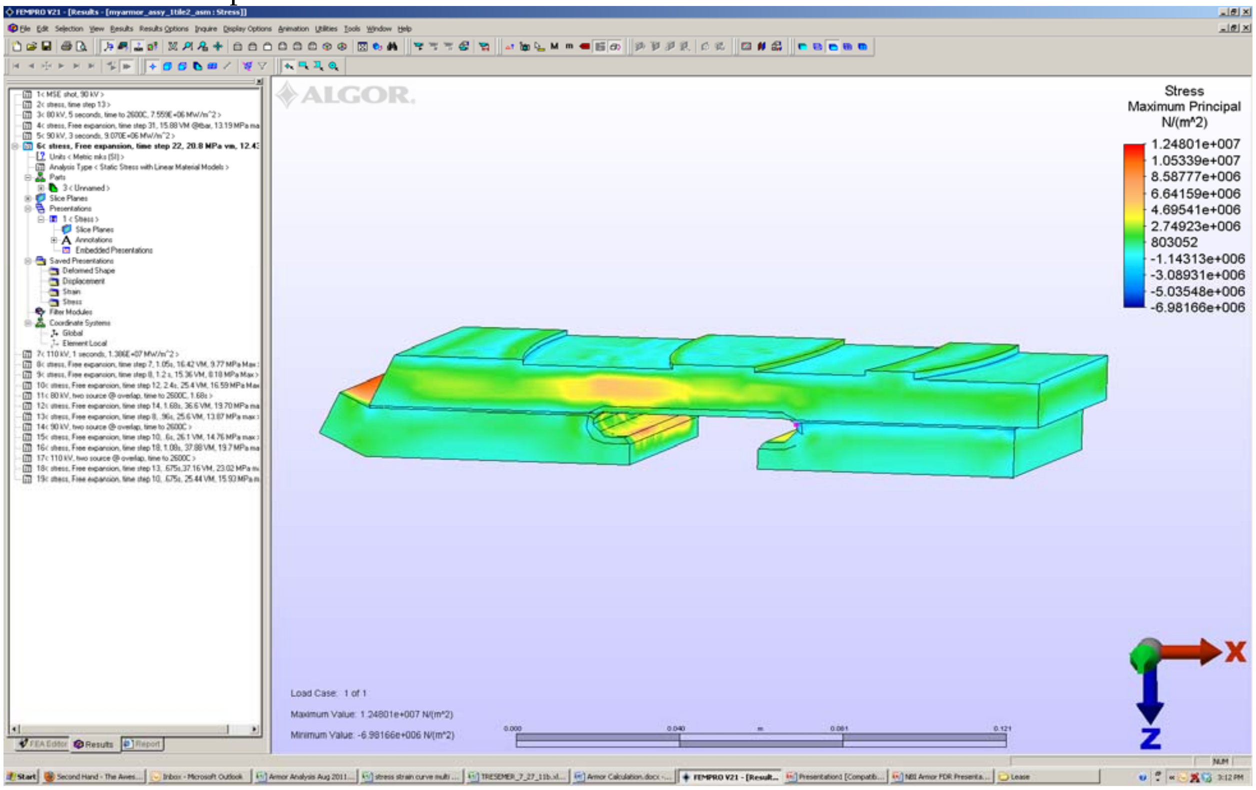

110 kV, 1s

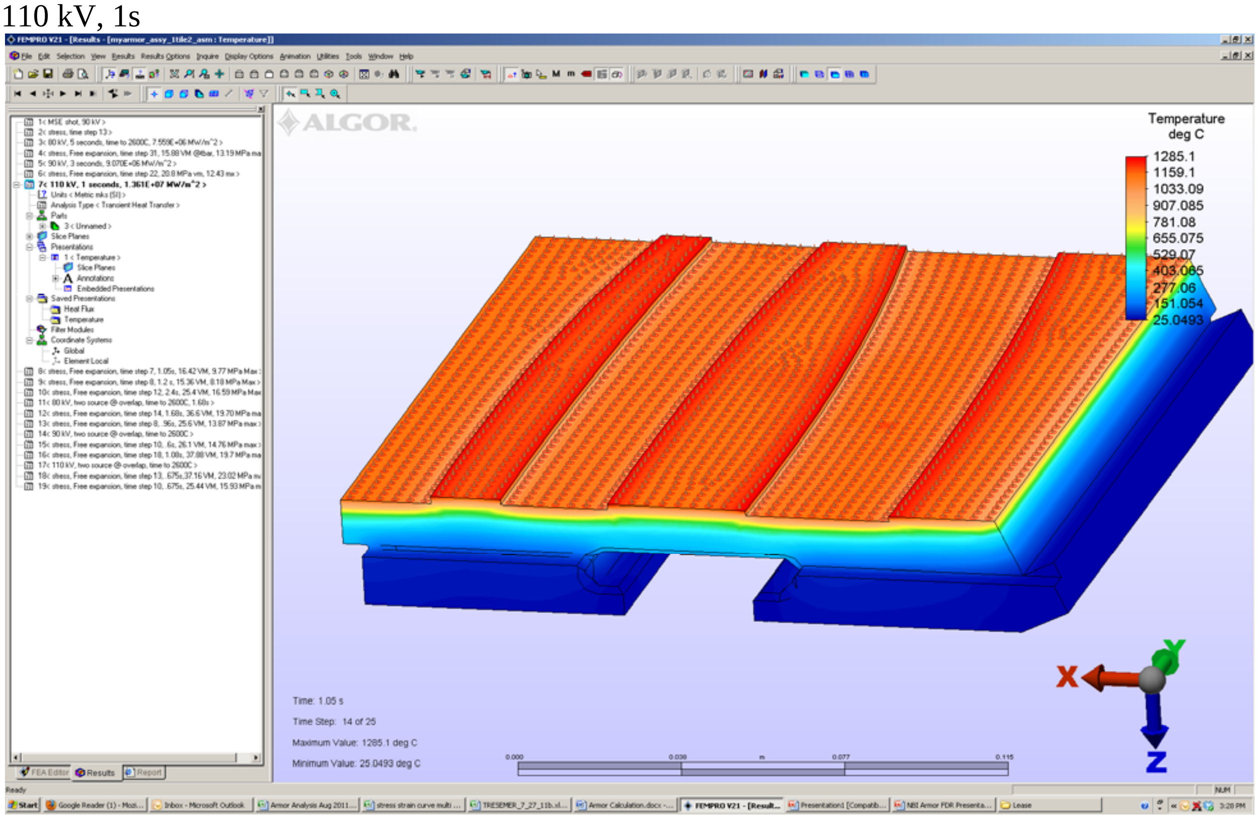

110 kV, Von Mises Stress

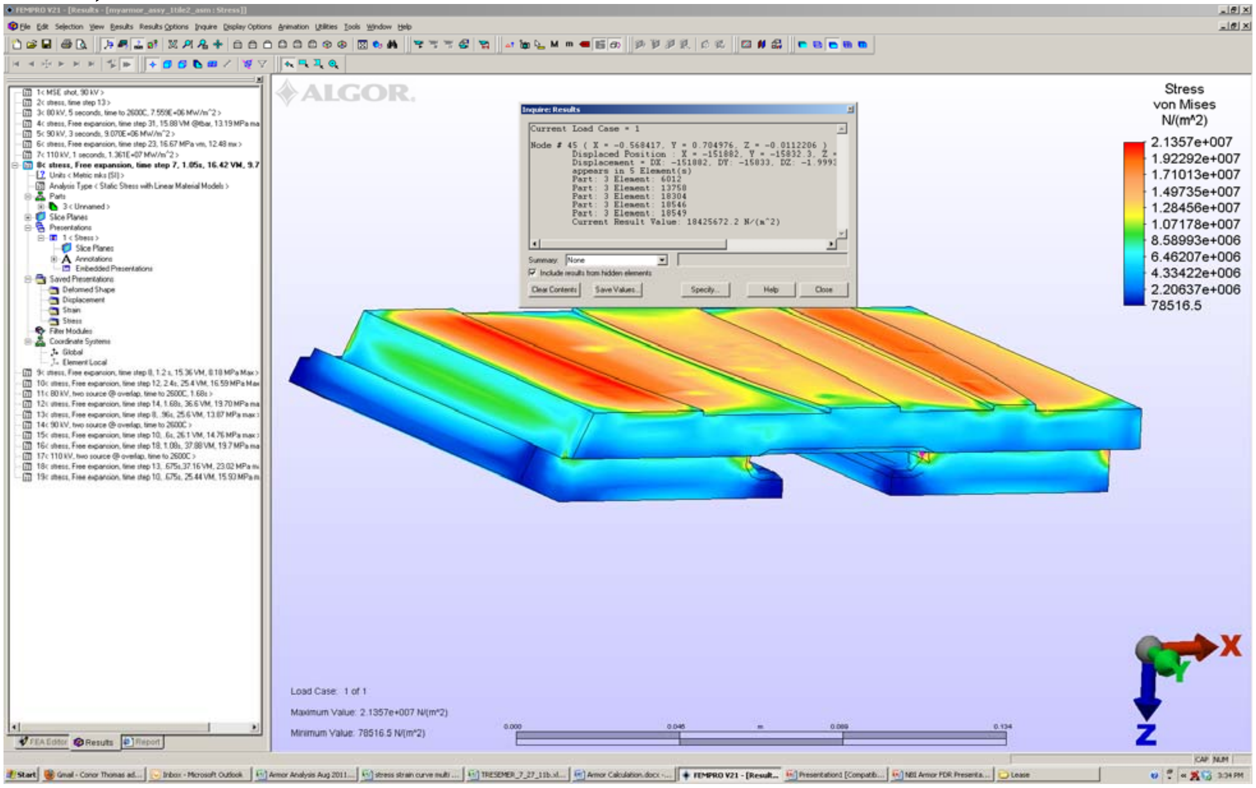

110 kV, Max Principle Stress

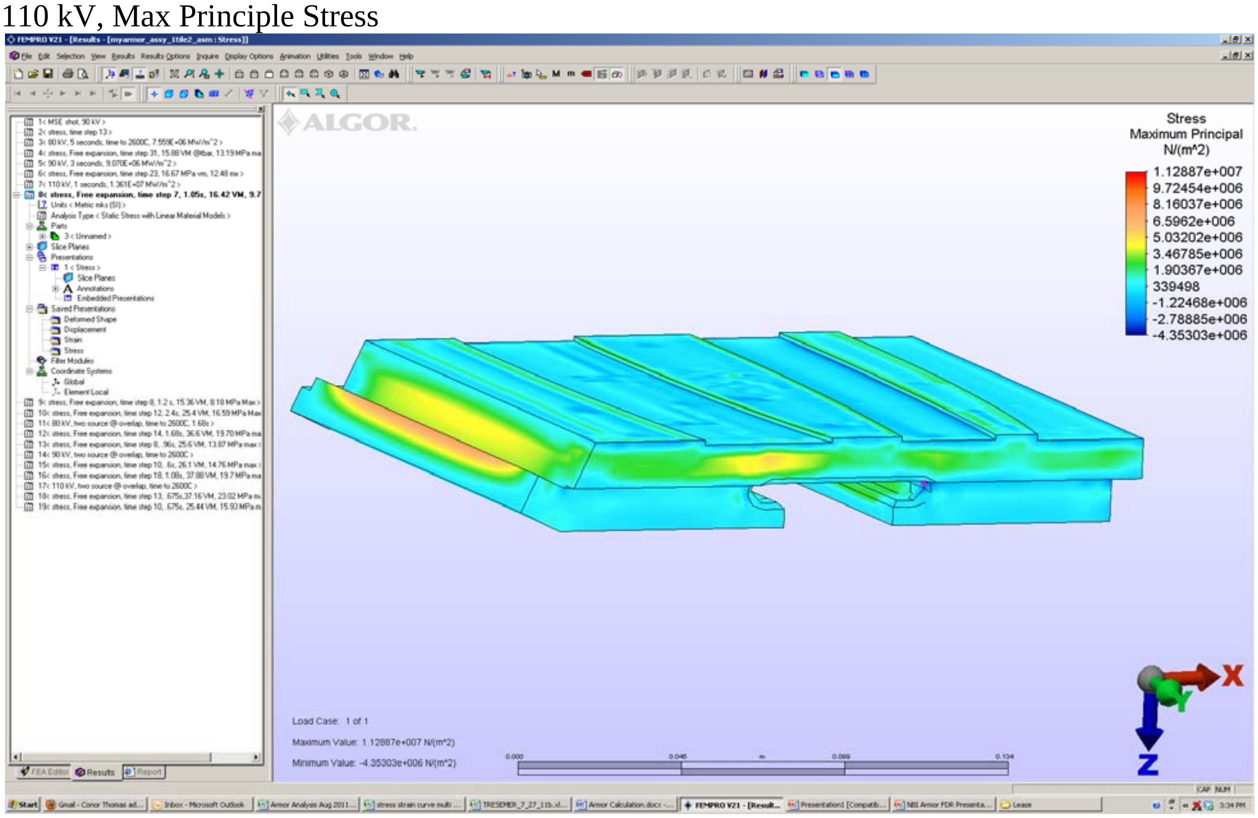

80 kV, 2 BL @ 2600C

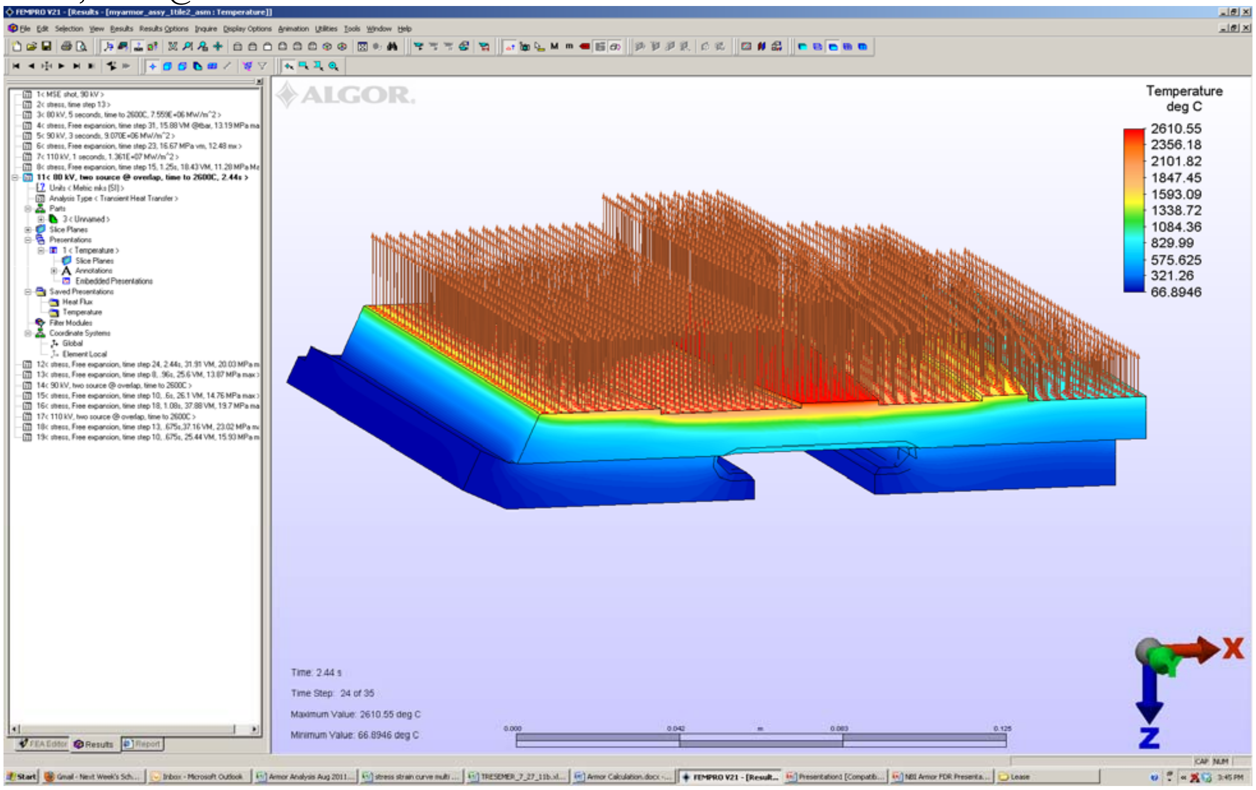

80 kV, 2 BL @ 2600C, Von Mises

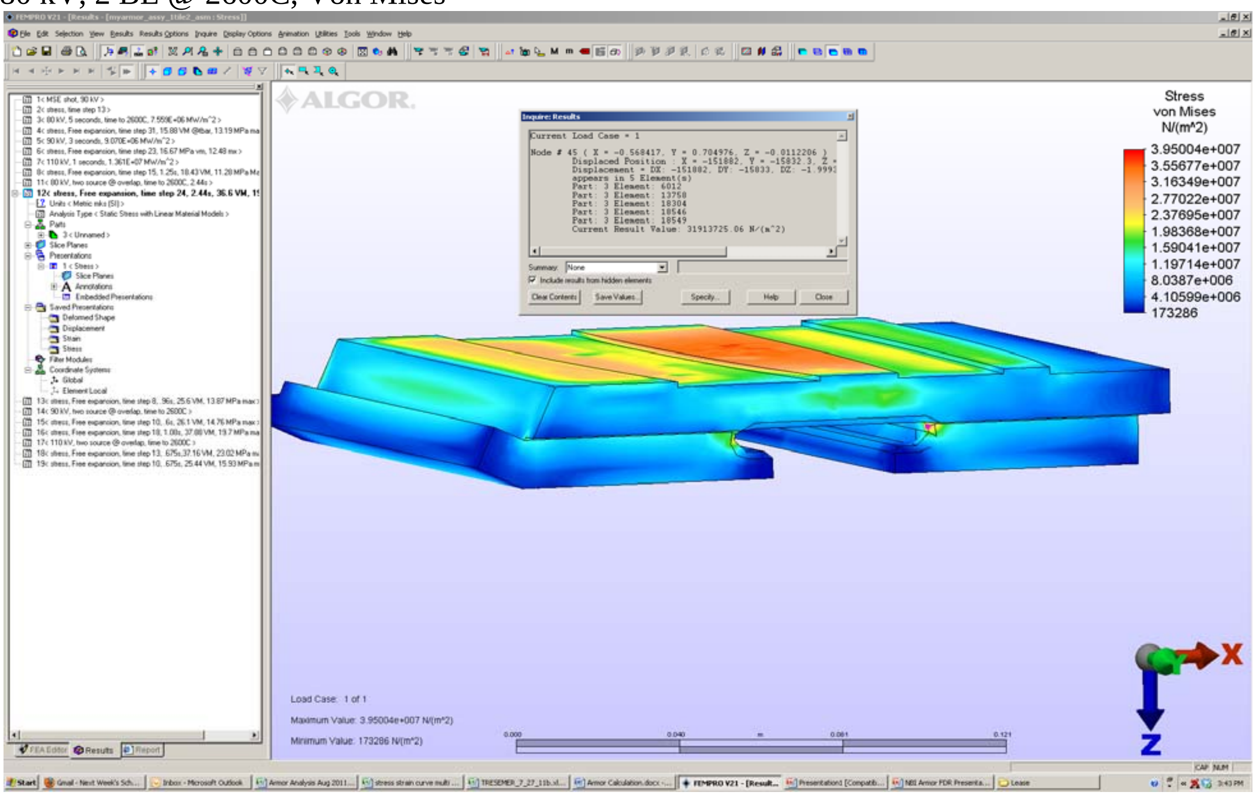

80 kV, 2 BL @ 2600C, Max Principle

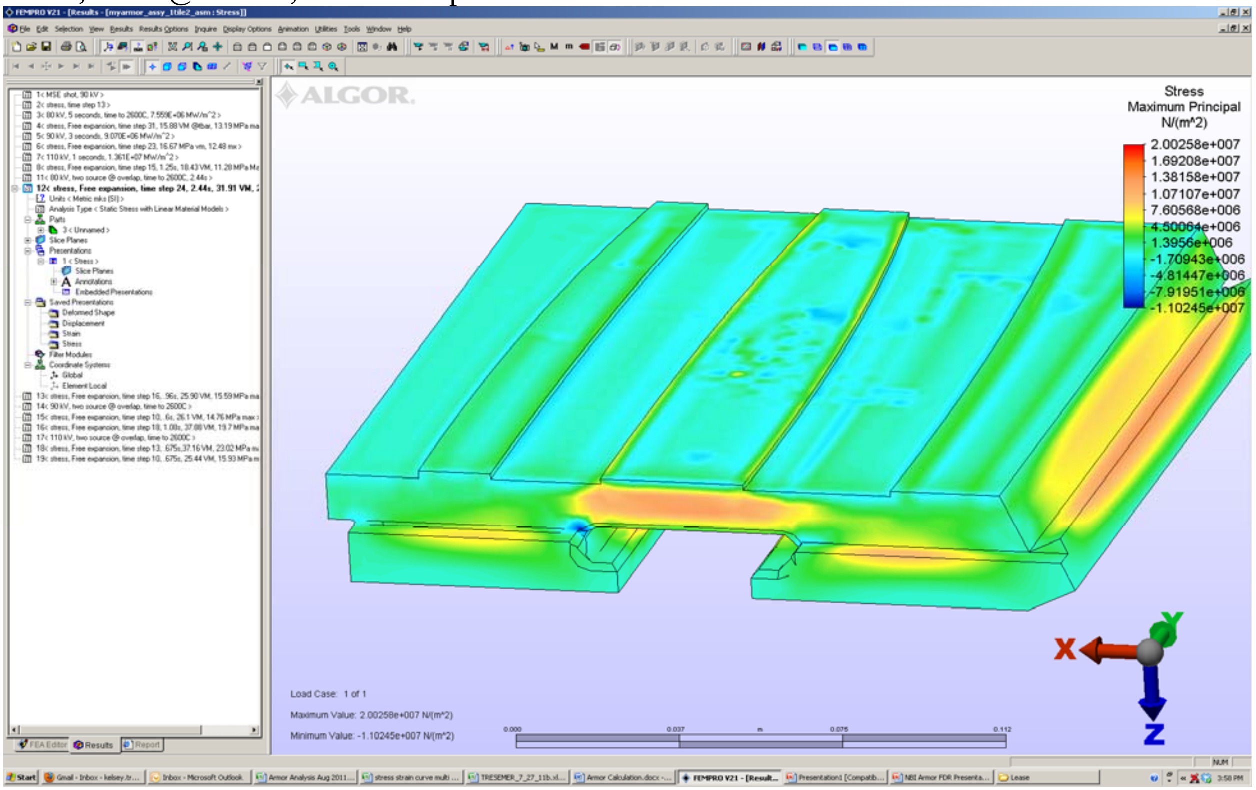

80 kV, 2 BL @ 26 Mpa Von Mises

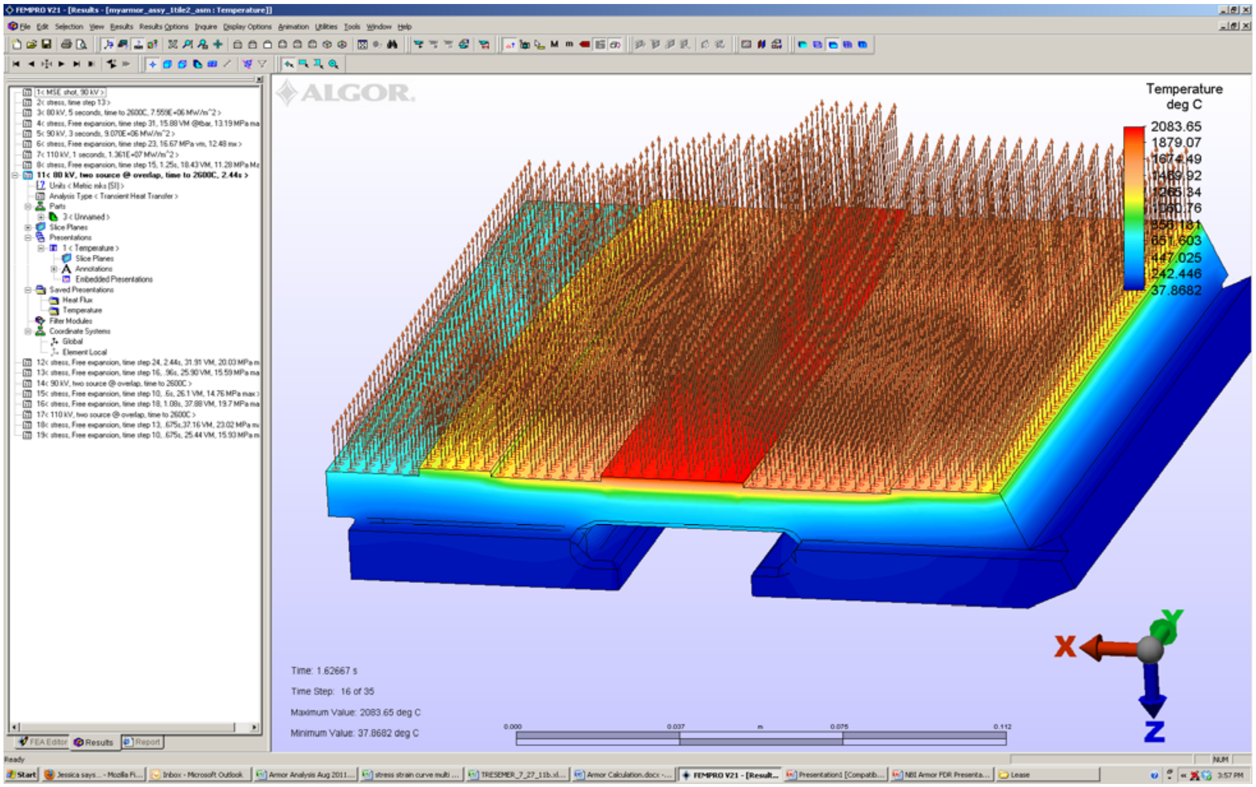

80 kV, 2 BL @ 26 Mpa Von Mises

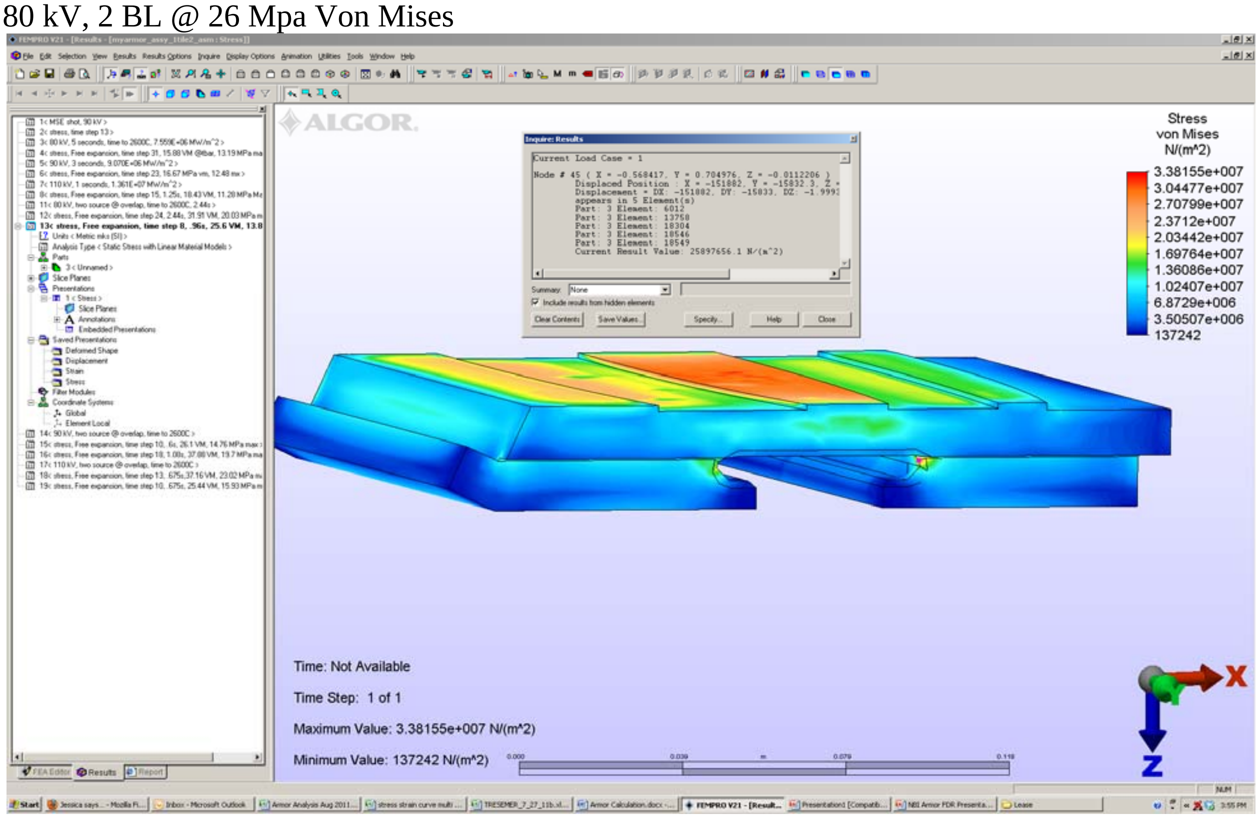

80 kV, 2 BL @ 26 Mpa Von Mises, Max Principle

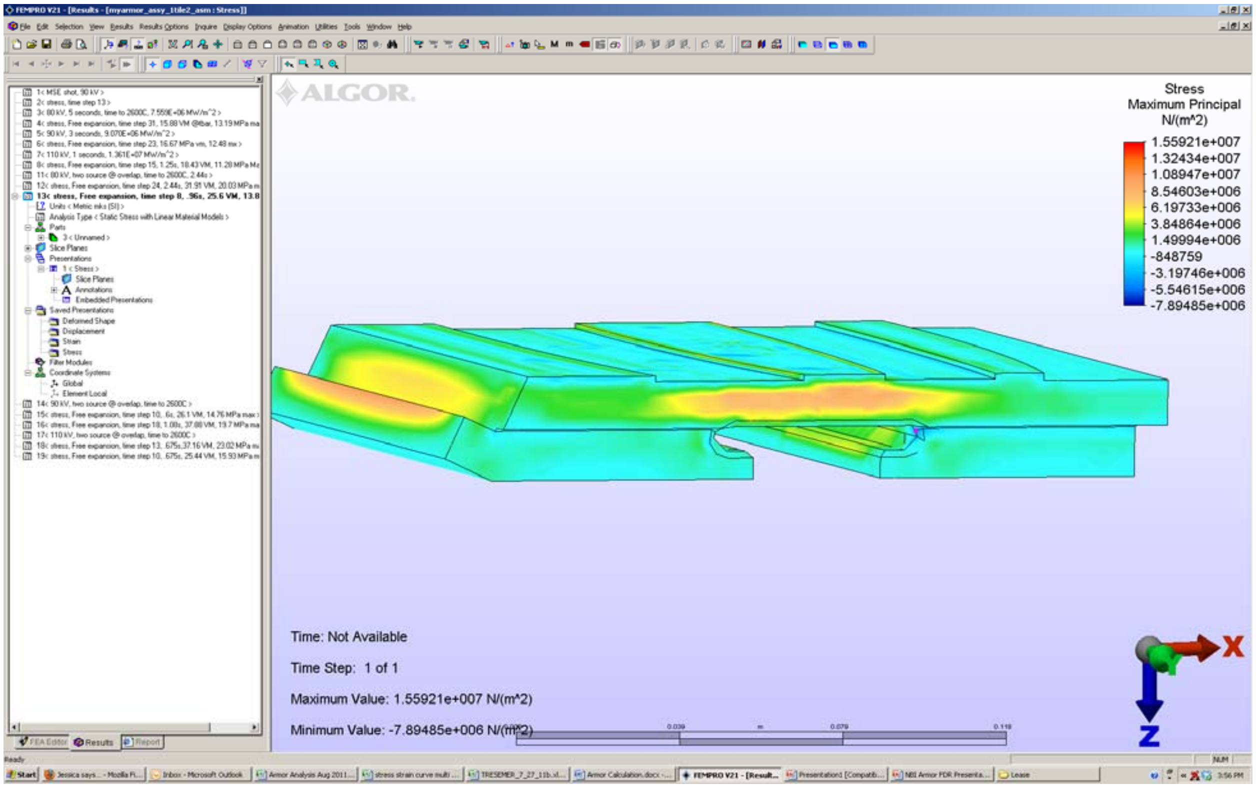

90 kV, 2 BL @ 2600 C

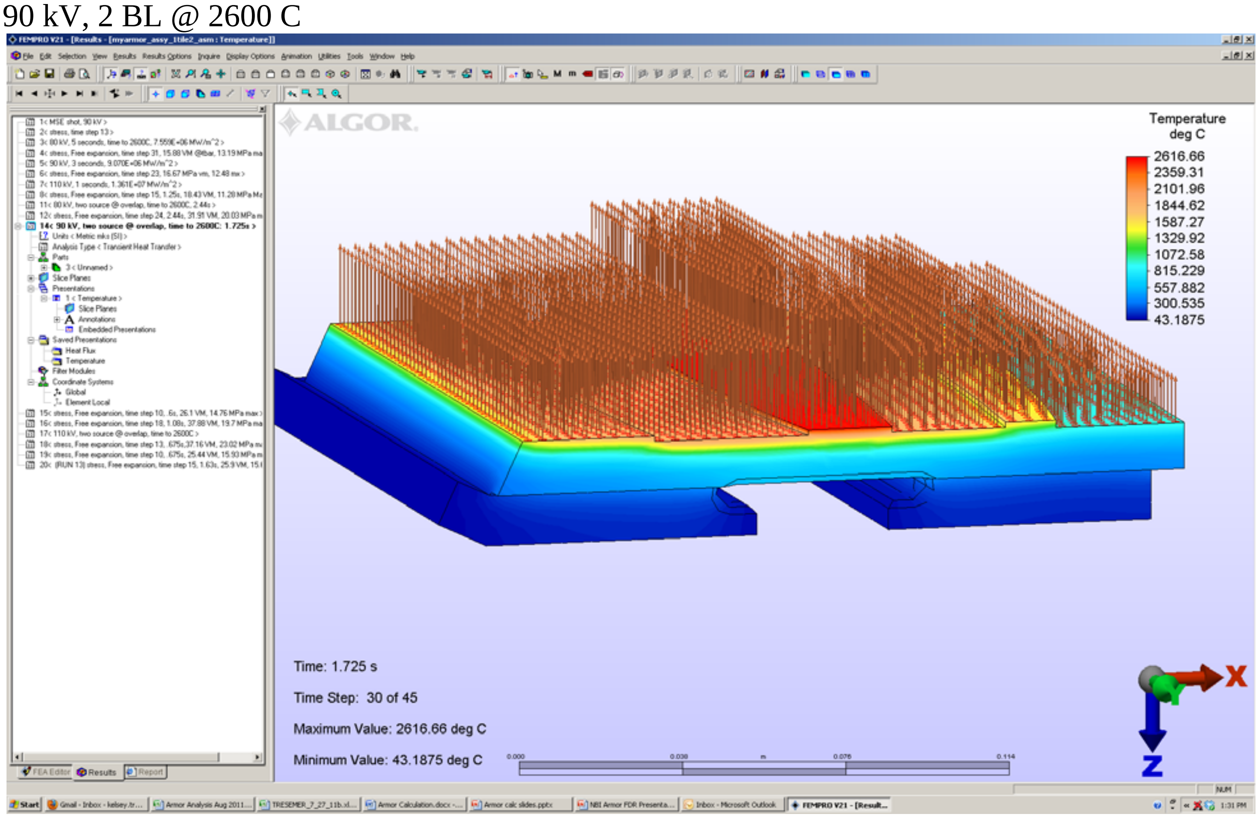

90 kV, 2 BL @ 2600 C, Von Mises

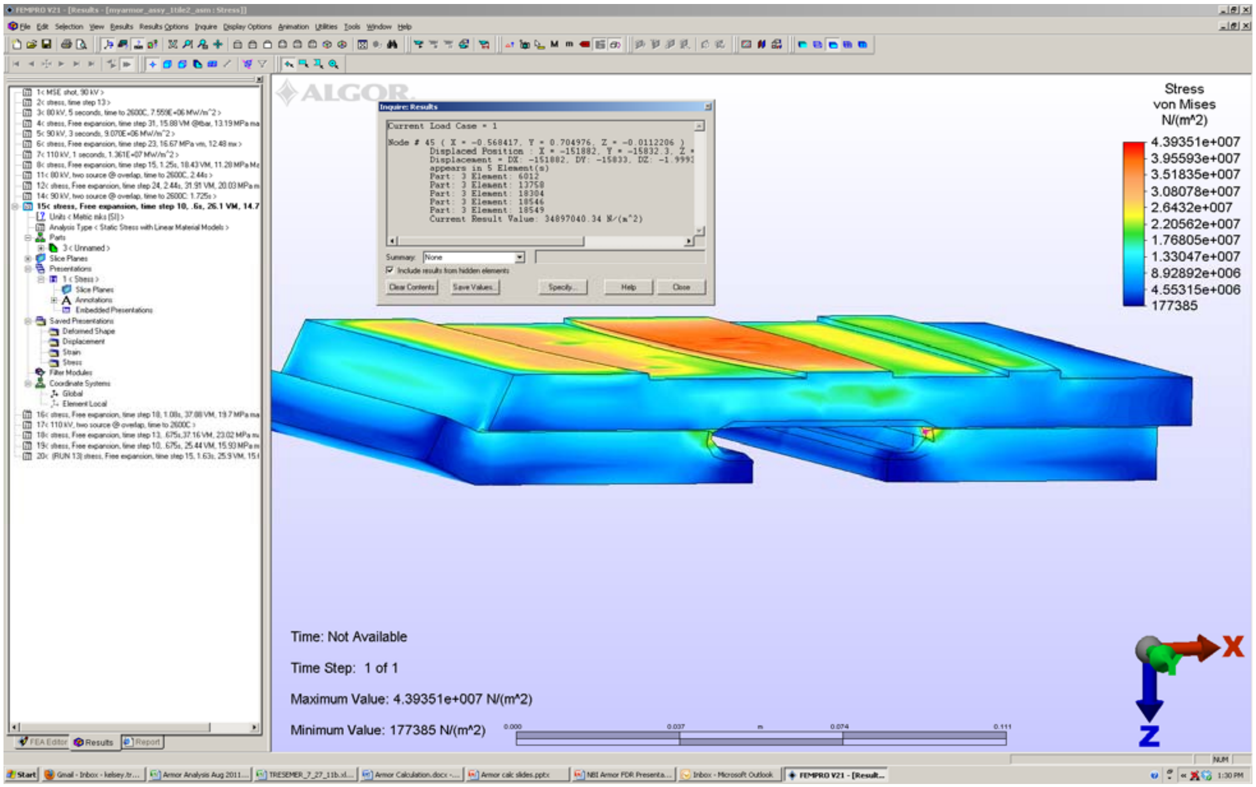

90 kV, 2 BL @ 2600 C, Max Principle

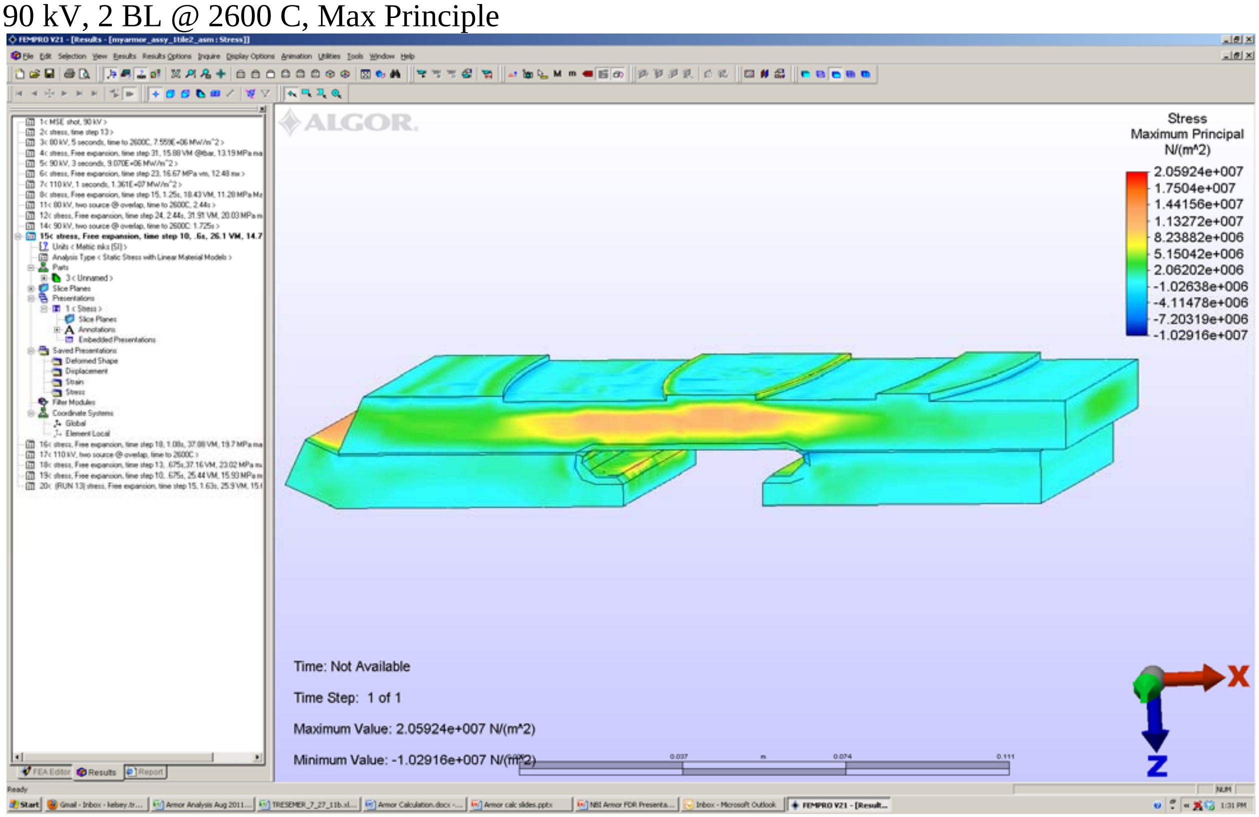

90 kV, 2 BL @ 26 Mpa Von Mises

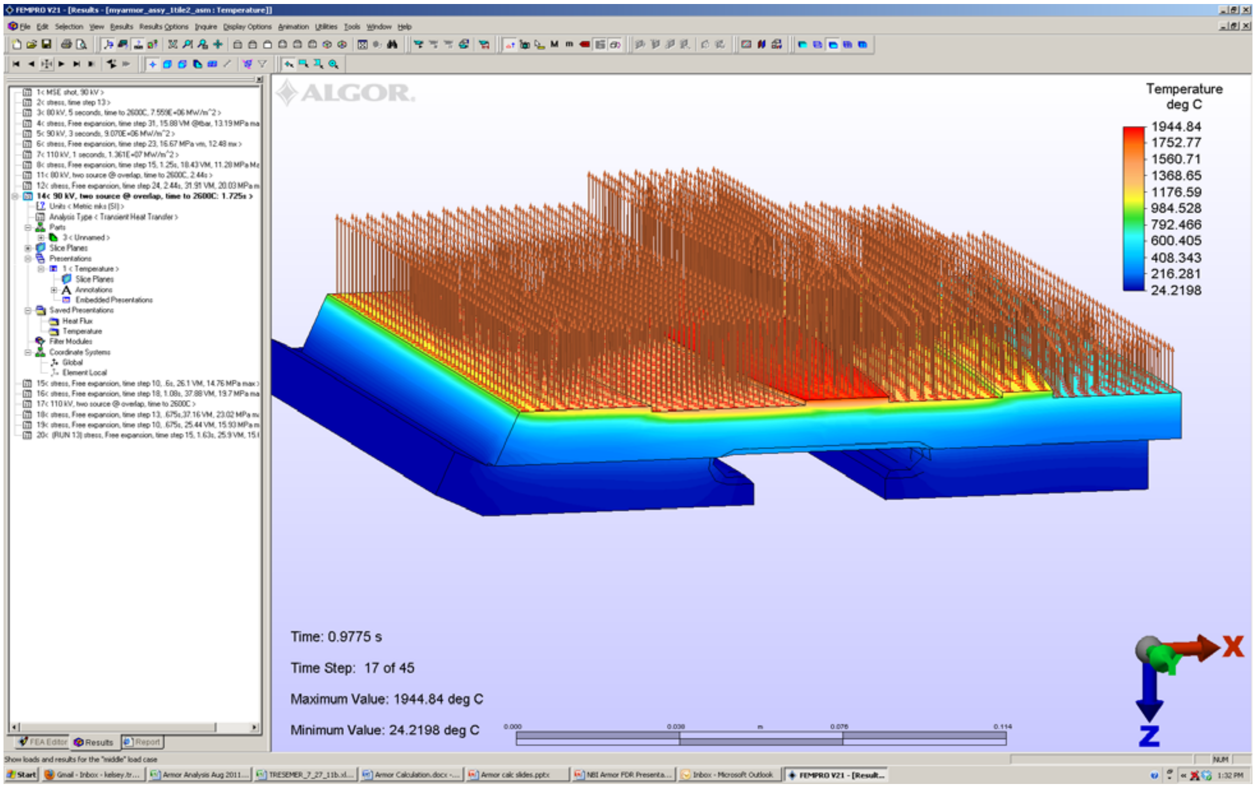

90 kV, 2 BL @ 26 Mpa Von Mises

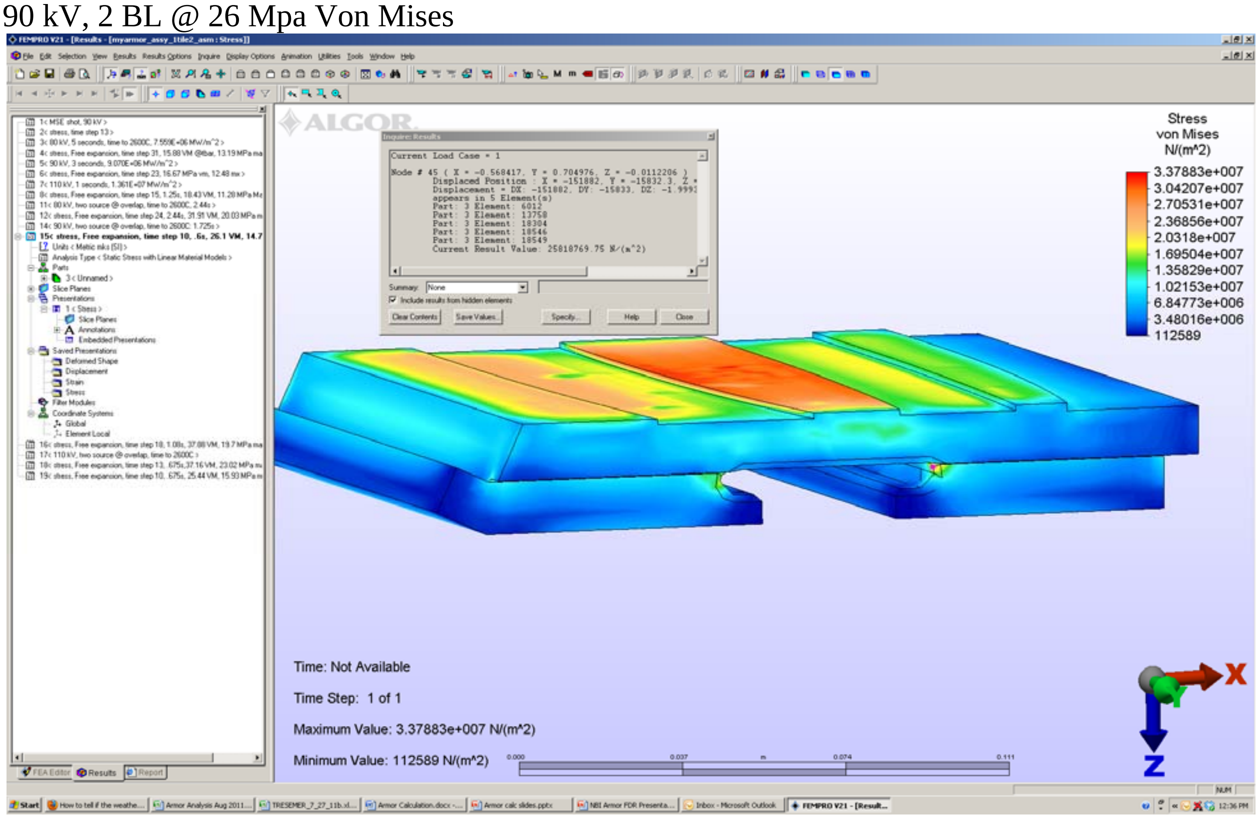

90 kV, 2 BL @ 26 Mpa Von Mises, Max Principle

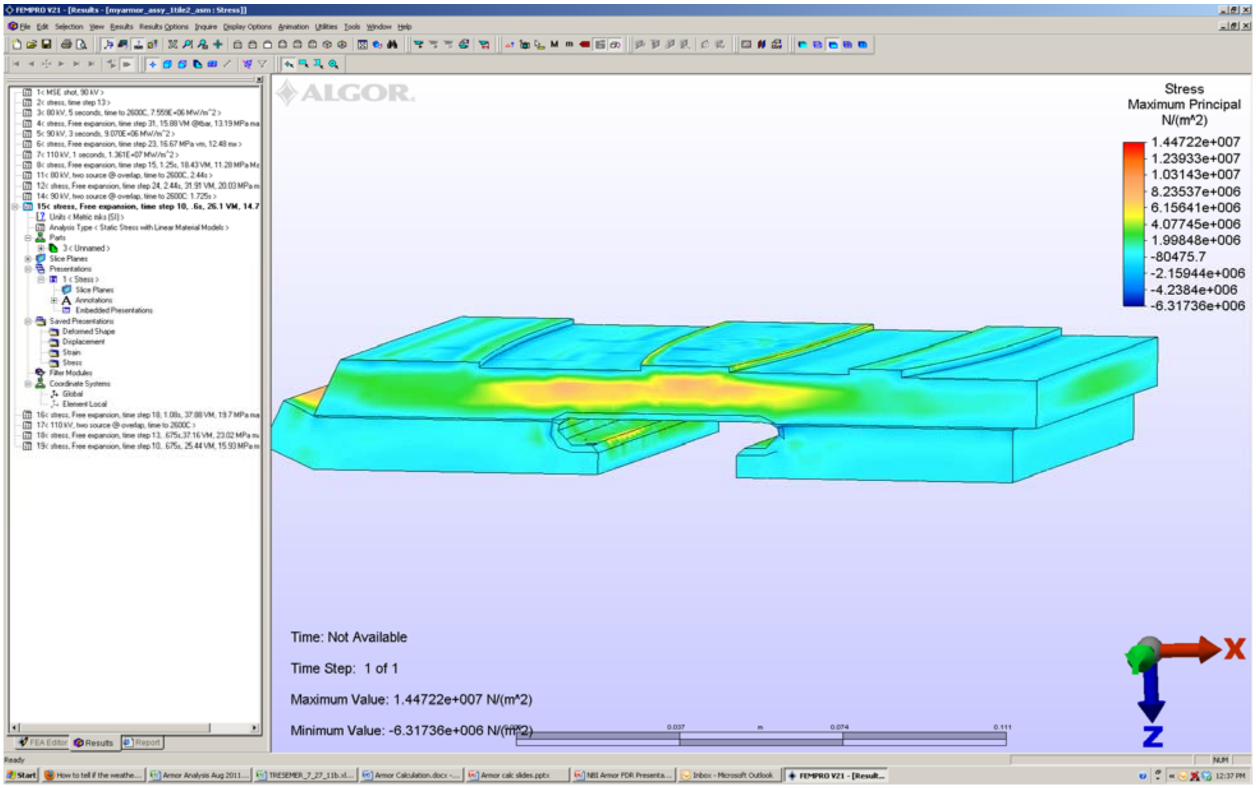

110 kV, 2 BL @ 2600 C

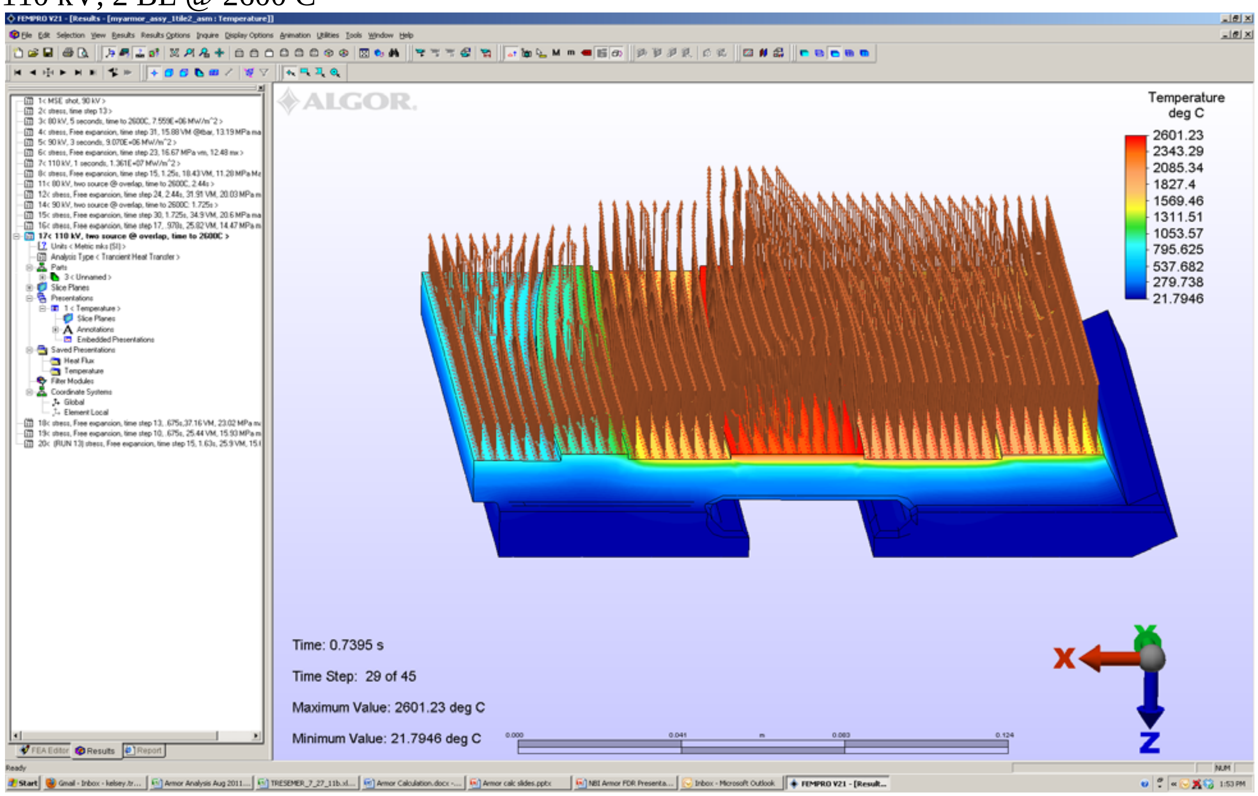

110 kV, 2 BL @ 2600 C, Von Mises

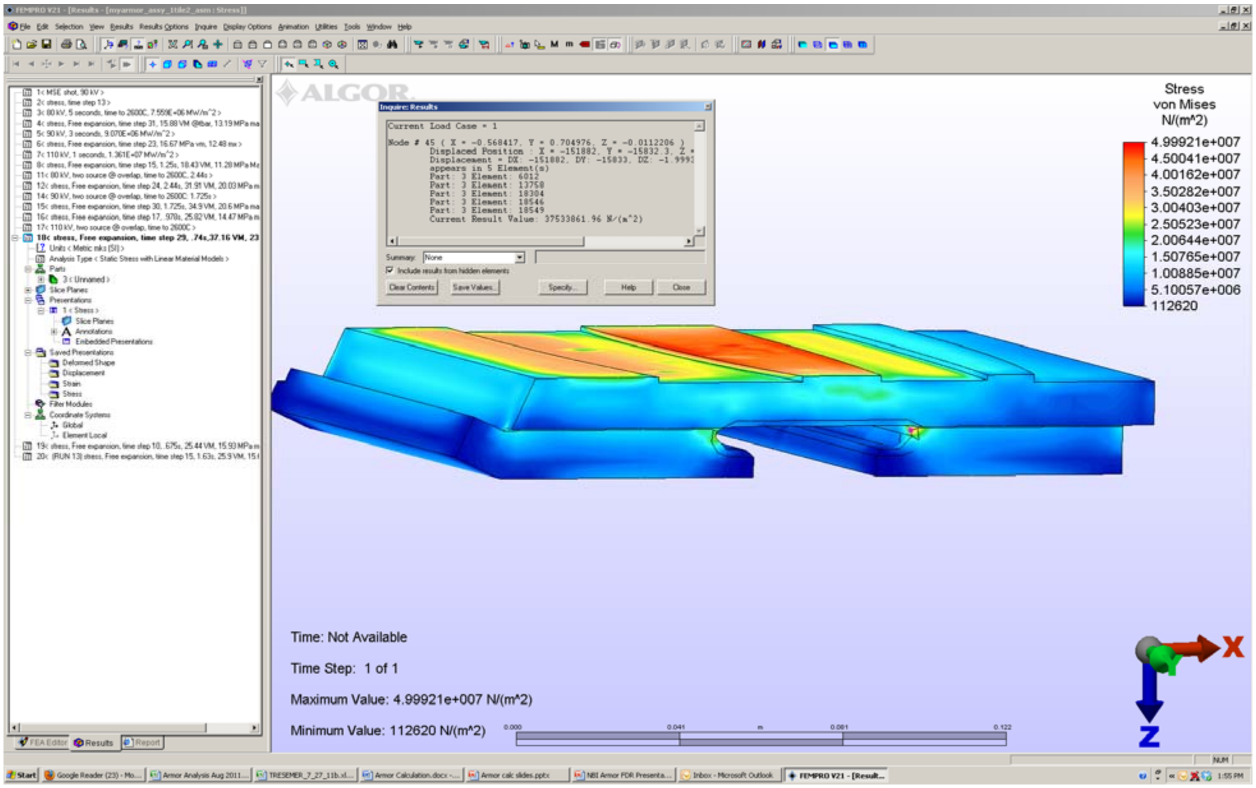

110 kV, 2 BL @ 2600 C, Max Principle

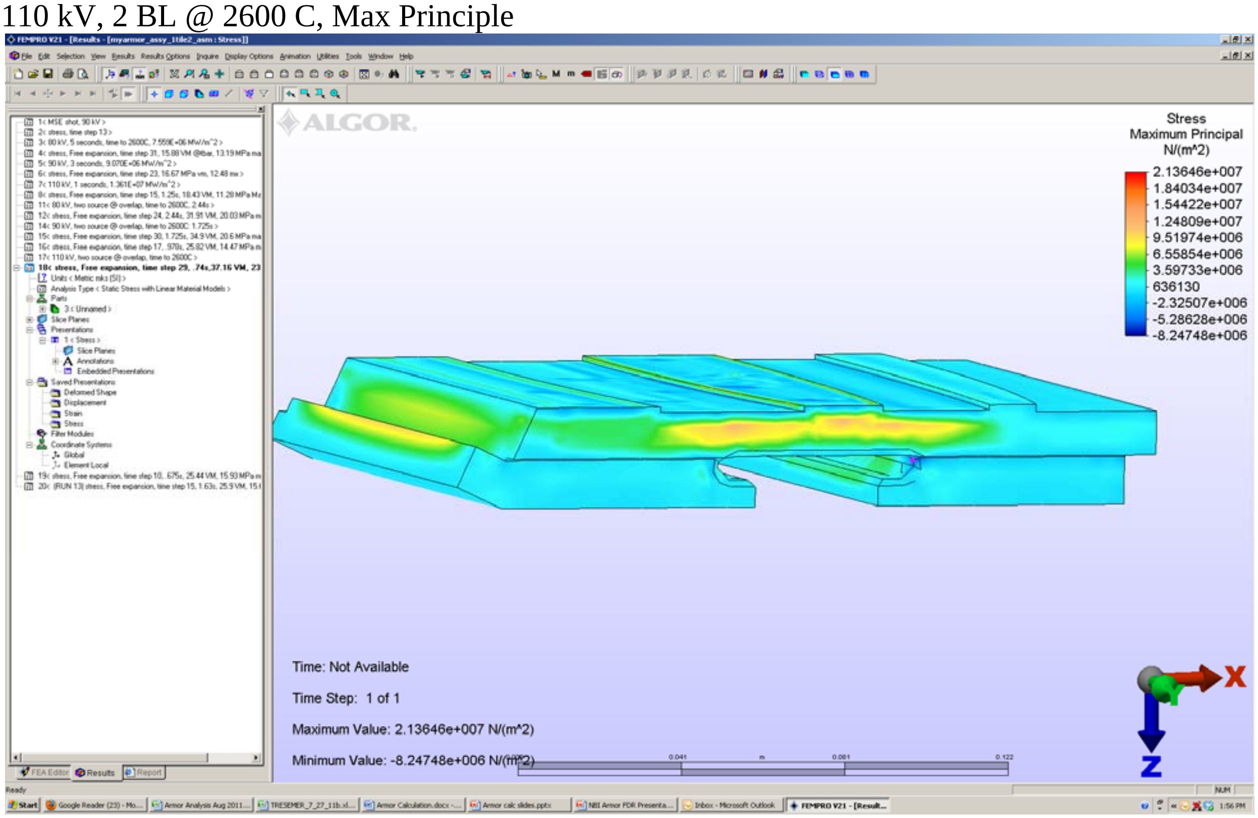

110 kV, 2 BL @ 26 Mpa Von Mises

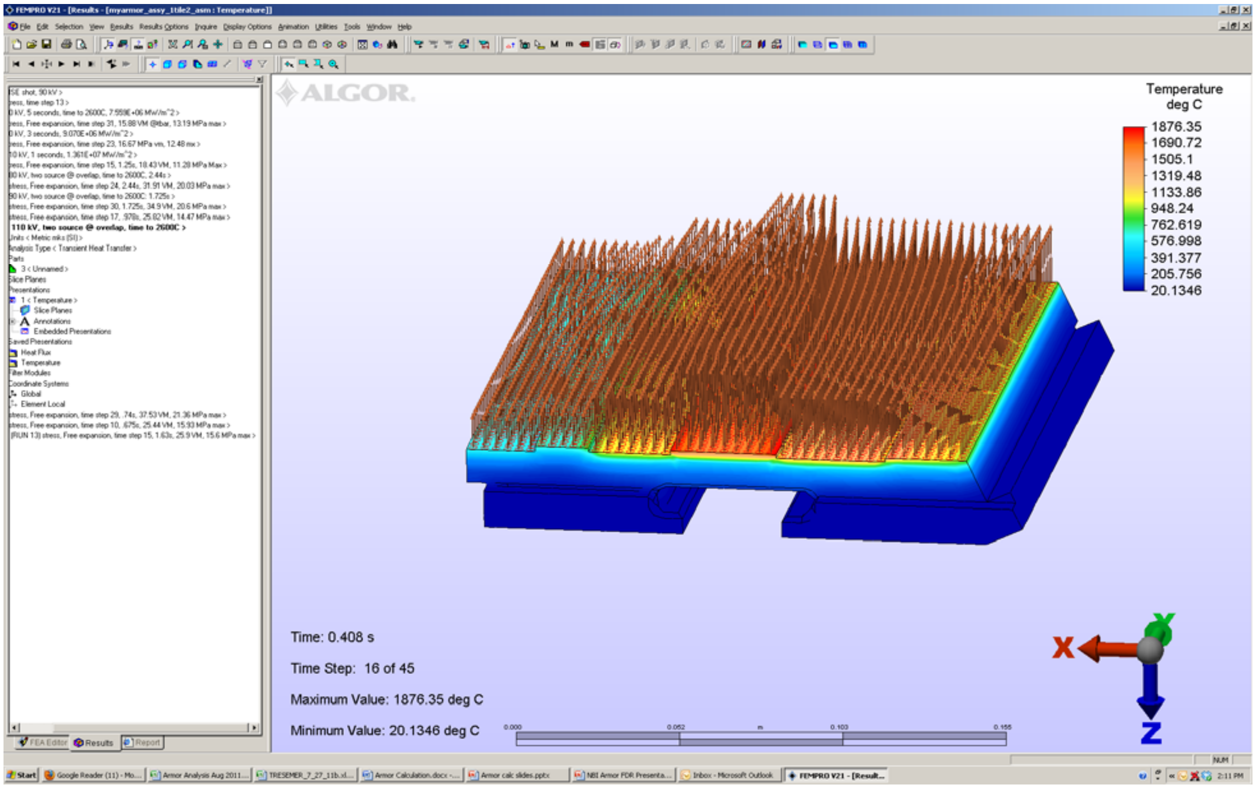

110 kV, 2 BL @ 26 Mpa Von Mises

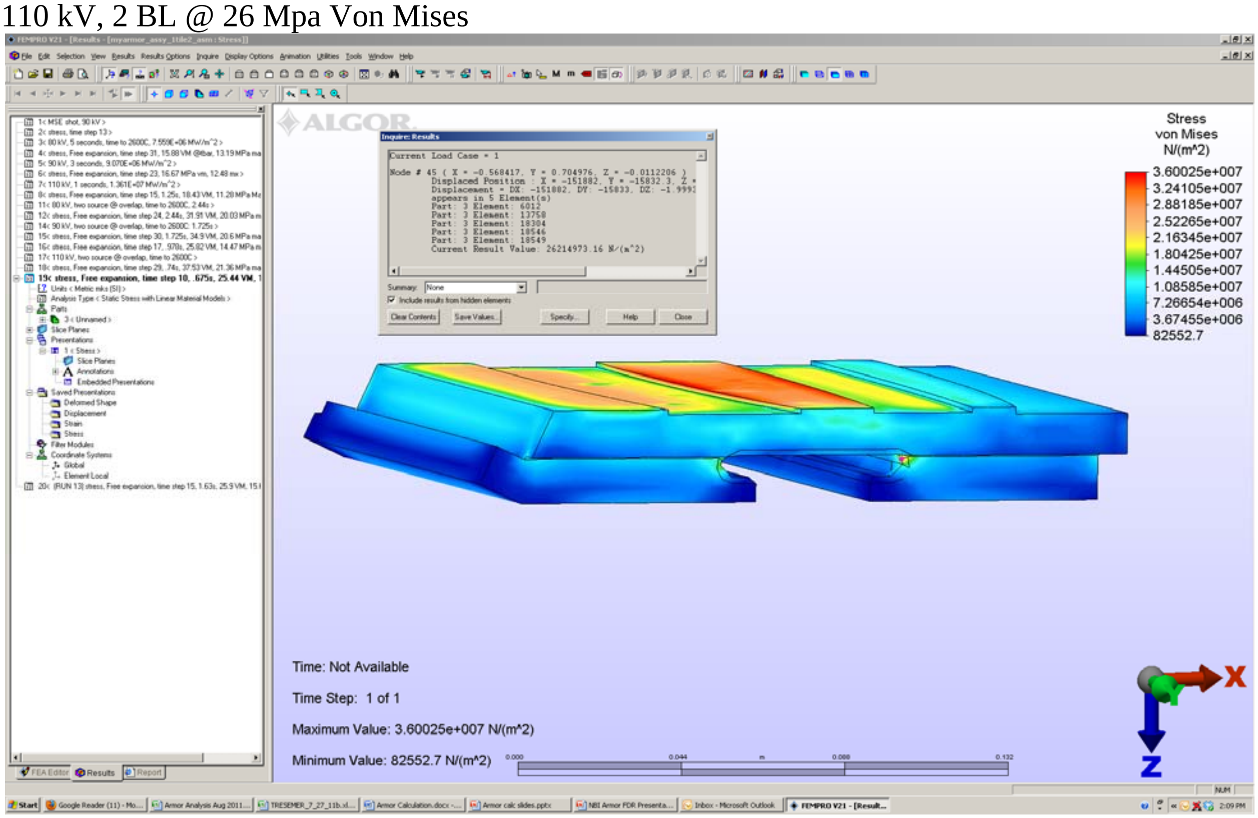

110 kV, 2 BL @ 26 Mpa Von Mises, Max Principle

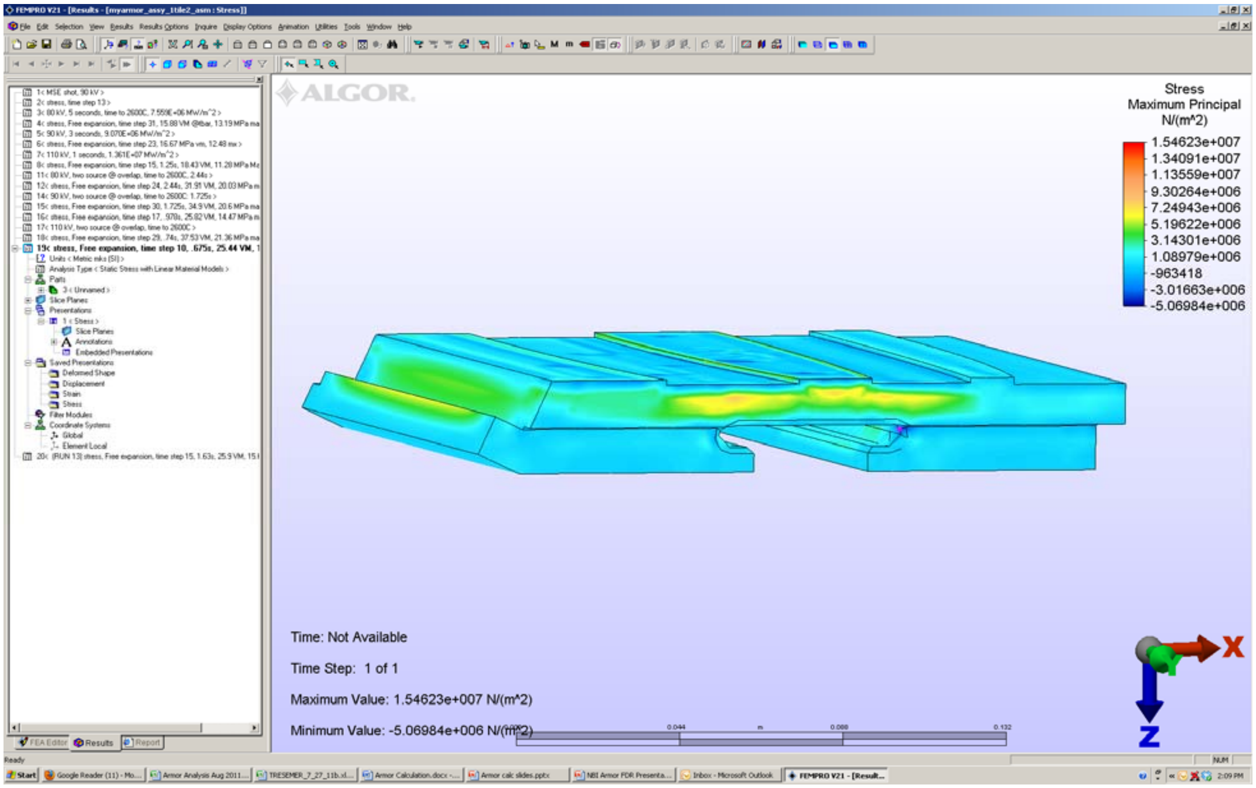

Cognizant Engineer's printed name, signature, and date

____

I have reviewed this calculation and, to my professional satisfaction, it is properly performed and correct.

Checker's printed name, signature, and date

____